Applied and Computational Mathematics
2024; 14(1): 37-63
http://www.sciencepublishinggroup.com/j/acm
doi: 10.11648/j.acm.20251401.14
ISSN: 2328-5605 (Print); ISSN: 2328-5613 (Online)

An Age-stratified Mathematical Model for Human Immunodeficiency Virus and Tuberculosis Co-infection with Optimal Control

Robert Mureithi Maina[1, *], Mathew Ngugi Kinyanjui[1], Samuel Musili Mwalili[1, 2], Duncan Gathungu Kioi[1]

[1]Pure and Applied Mathematics, Jomo Kenyatta University of Agriculture and Technology, Nairobi, Kenya
[2]Strathmore Institute of Mathematics, Strathmore University, Nairobi, Kenya

Email address:

mainarobert16@gmail.com (Robert Mureithi Maina), mathewkiny@jkuat.ac.ke (Mathew Ngugi Kinyanjui), smwalili@strathmore.edu (Samuel Musili Mwalili), dkioi@jkuat.ac.ke (Duncan Gathungu Kioi)
*Corresponding author

To cite this article:

Robert Mureithi Maina, Mathew Ngugi Kinyanjui, Samuel Musili Mwalili, Duncan Gathungu Kioi. (2025). An Age-stratified Mathematical Model for Human Immunodeficiency Virus and Tuberculosis Co-infection with Optimal Control. *Applied and Computational Mathematics, 14*(1), 37-63. https://doi.org/10.11648/j.acm.20251401.14

Received: 17 December 2024; **Accepted:** 2 January 2025; **Published:** 14 January 2025

Abstract: One significant risk factor that is considered to contribute to Kenya's TB burden is HIV. TB is one of the most common opportunistic infections associated with HIV, and HIV infection increases the risk of developing active TB disease in individuals with latent TB infection. Due to their compromised immune systems, increased susceptibility to TB infection and latent TB reactivation, people with HIV have a higher probability of attaining TB. This study develops an age-stratified mathematical model with optimal control for co-infection of HIV and TB. The model's reproduction number, as well as the equilibrium of endemic and disease-free states have been computed. Least Squares technique of minimization has be used to determine the model parameters. HIV antiretroviral therapy treatment adherence and tuberculosis treatment have been considered for optimization. Runge-Kutta $\mathcal{O}(h^4)$ has been used to solve the system differential equations for its high accuracy and flexibility. Results from the numerical simulations show that ART adherence is the best intervention to control the co-infection in its earlier stages (HIV and latent TB). TB treatment is the best intervention for those affected with the coinfection on the later stage (HIV and active TB). Considering viral load suppression and TB prevention, viral load suppression is most effective for children and TB prevention is most effective for adults. The results of this research can be used by the Ministry of Health (MOH) for emphasis on most effective interventions as well as a basis study tool that can be recreated for other co-infections.

Keywords: Age-stratified, Co-infection, Optimal Control

1. Introduction

HIV is transmitted through certain body fluids, including blood, semen, vaginal fluids, and breast milk [1]. The most common modes of transmission include unprotected sexual intercourse, sharing needles or syringes contaminated with HIV-infected blood, and from mother to child during childbirth or breastfeeding [2]. Tuberculosis (TB) is an infectious disease caused by the bacterium *Mycobacterium tuberculosis*. TB is primarily spread through the air when an infected person coughs, sneezes, or talks, releasing tiny droplets containing the bacteria [3].

HIV-TB coinfection occurs when an individual is infected with both HIV (Human Immunodeficiency Virus) and TB (Tuberculosis). HIV-TB coinfection can have synergistic effects, with each disease exacerbating the progression and severity of the other. HIV infection raises the chance of developing active TB disease in those with latent TB infection, and TB is one of the most prevalent opportunistic infections linked to HIV. HIV-positive individuals are more likely to develop TB because of weakened immune systems, increased vulnerability to TB infection, and latent TB reactivation [4].

HIV primarily targets CD4+ T cells, which are essential for TB infection control, weakening the immune system. As a result, those who have HIV are less able to control the TB germs, which causes the TB condition to progress more quickly. Co-infected individuals may have more severe and rapid progression of both HIV and TB, leading to increased morbidity and mortality if not diagnosed and treated promptly. Diagnosis and treatment of HIV-TB co-infection require careful coordination and management, including simultaneous treatment of both diseases and monitoring for drug interactions and potential complications [5].

Since the first case was identified in 1984, the HIV epidemic in Kenya has progressed to rank among the leading causes of death and has put enormous strain on the country's health system and financial resources [6]. Antiretroviral therapy (ART), a medication used to treat HIV, slows the progression of the illness by preventing the virus from replicating in the body. In Kenya, tuberculosis (TB) is a serious public health concern that presents difficulties for both communities and healthcare systems across. Kenya and other SubSaharan African countries are among those with a high worldwide TB burden. Each year, more than 120,000 people contract TB, with about 11% of cases occurring in children. According to estimates from Kenya's Ministry of Health, TB caused 3.2% of all fatalities in 2020 [7].

According to the [4], Kenya has emphasized efforts to treat HIV/TB coinfection since HIV infection significantly rises the incidence of active tuberculosis to patients who are dually infected. Kenya was the first country in sub-Saharan Africa to meet the worldwide targets for identification of tuberculosis cases at 80% and treatment rate at 85%. The percentage of TB patients who were tested for HIV increased from 83% in 2008 to 95% in 2009, exceeding the set national target which of 90% TB cases being tested in 2013.

A study on Rural Kenyan TB patients' HIV burden and treatment outcomes showed despite the strong uptake of antiretroviral therapy (ARTs) and cotrimoxazole preventative medicine, HIV infection and unknown HIV status were linked to reduced TB treatment completion rates, a higher risk of death, and TB treatment default [8]. This result emphasized the need for greater study on methods targeted at finishing TB treatment and reducing death. A nonlinear compartment model was used to assess the impact of media coverage on the control and prevention of HIV/AIDS and tuberculosis [9]. The study concluded that if TB infection is treated properly then HIV infection can be kept under control. A comprehensive review and meta-analysis study to determine the combined burden of virological unsuppression among individuals with HIV-TB and the impact of TB on virological failure in Ethiopia by [10] suggested stepping up efforts to prevent tuberculosis, managing cases as soon as they are identified, and giving adult HIV-positive individuals' viral load monitoring and adherence assistance should be a top priority.

According to KENPHIA report [11], the estimated HIV prevalence in Kenya for adults aged $15-49$ is 4.5%. In contrast to the 5% national HIV prevalence, the rates for those aged $50-54$, $55-59$, and $60-64$ were 9%, 8%, and 6%, respectively. Individuals who received *HIV Testing* and received results were 64.4% for $15-24$ years, 87.9% for $25-49$ years, 74.6% for $50-64$ years and 78.5% for $15-49$ years. HIV positive status on *ART treatment*; 49.1% for $15-24$ years, 67.2% for $25-49$ years, 80.8% for $50-64$ years and 65.0% for $15-49$ years.

From the discussed previous work done, it is evident that there needs to be more study on the effectiveness of the different interventions put forward to control HIV-TB co-infection. This study develops an age-stratified mathematical model which has not been addressed by the previous studies covered. This research paves way to helpful insights and ideas which will impact positively in Kenya's fight of infectious diseases.

2. Materials and Methods

In this section, a deterministic mathematical model is developed to analyze the transmission dynamics of the HIV and TB co-infection. Model analysis is performed to check the model's well-posedness. The model is the subdivided to three sub-models; HIV, TB and Full model. The equilibrium states are computed and both local and global stability of the sub-models is proved. Finally, the methods of solution are presented.

2.1. Model Formulation

Various assumptions were made to simplify the complexity of the disease interaction and to focus on specific aspects of the problem. The risk of an individual contracting an infection is not influenced by factors such as gender, social status, race, or environmental factors. Individuals in the population have an equal chance of encountering and transmitting the infection to others. Drug resistance is asumed. Other health conditions that can influence disease outcomes and treatment responses are assumed. The population is considered to be mixing uniformly (homogeneous) [12]. The entire population $N(t)$ is split into multiple epidemiological states at any given time t.

This study partitioned Kenyan population into 2 groups according to available data from UNAIDS and National Tuberculosis, Leprosy and Lung Disease Program (NLTP); children $0-14$ years, and adults above 15 years. Each group is labeled by subscript $i=1,\ 2$ respectively. Each population of age group i is classified into ten compartments. The model has this classes: The susceptible individuals $S_i(t)$ are recruited at rate π. These class can be infected with HIV and be undiagnosed $U_i(t)$ or Latent TB infected $E_i(t)$. It is assumed that individuals infected with HIV become Diagnosed $D_i(t)$ at a rate ϵ_i. These individuals can get recruited under anti-retroviral therapy class $A_i(t)$. Individuals in the $A_i(t)$ may drop out of art at rate d_i and join class $D_i(t)$. Individuals infected with Latent TB can advance to Active TB $I_i(t)$ or treated to join the Treatment class $R_i(t)$ [13]. Treated Active TB individuals can be reinfected with TB at a rate θ to join E_i. Individuals can either have co-infection of undiagnosed HIV and Latent TB, C_{LUi}, diagnosed HIV and Latent TB, C_{LHi} or HIV and Active TB, C_{THi}

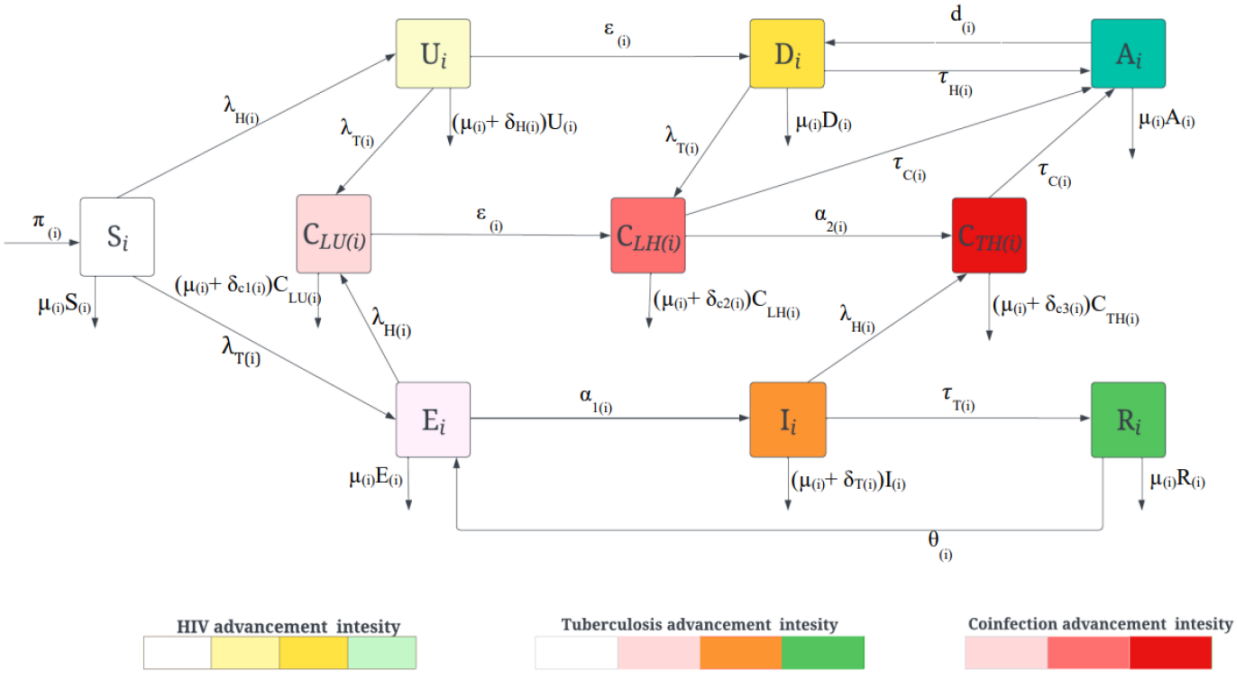

Figure 1. *Parameterized compartmental model for HIV and TB co-infection.*

Table 1. *Model parameters.*

Parameters	Epidemiological Interpretation
$\pi_{(i)}$	Recruitment rate for susceptible individuals
$\beta_{H(i)}$	Transmission rate for HIV respectively
$\beta_{T(i)}$	Transmission rate for TB respectively
$\mu_{(i)}$	Natural mortality rate
$\epsilon_{(i)}$	Rate of HIV testing
$\alpha_{1(i)}$	Progression rate from latent to Active TB
$\alpha_{2(i)}$	Progression rate from $C_{LH(i)}$ to $C_{TH(i)}$
$\tau_{H(i)}$	Treatment rate of HIV infectives
$\tau_{T(i)}$	Treatment rate of TB infectives
$\tau_{C(i)}$	Treatment rate of TB-HIV co-infectives
$\theta_{(i)}$	TB treatment failure
$d_{(i)}$	Rate of ART dropout
$\eta_{(i)}$	Proportion of ART non-adherence
$\delta_{H(i)}$	Mortality induced by HIV only
$\delta_{T(i)}$	Mortality induced by TB only
$\delta_{C1(i)}$	Mortality induced by $C_{LU(i)}$
$\delta_{C2(i)}$	Mortality induced by $C_{LH(i)}$
$\delta_{C3(i)}$	Mortality induced by $C_{TH(i)}$

The total population $N_i(t)$ is given by;

$$N_i(t) = S_i(t) + U_i(t) + D_i(t) + A_i(t) + E_i(t) + I_i(t) \tag{1}$$

$$+ R_i(t) + C_{LUi}(t) + C_{LHi}(t) + C_{THi}(t), \tag{2}$$

The force of infection associated with HIV is given as,

$$\lambda_{H_i} = \frac{\beta_{H(i)}}{N}(U + D + \eta_i A + C_{LU} + C_{LH} + C_{TH})$$

Further, individuals infected with TB and those who are coinfected with HIV and TB can spread TB among susceptible individuals with the force of infection, given as,

$$\lambda_{T_i} = \frac{\beta_{T(i)}}{N}(I + C_{TH})$$

The differential equations based on the compartmental model and the parameter descriptions are provided by,

$$\begin{aligned}
\frac{dS_i}{dt} &= \pi_{(i)} - (\lambda_{H(i)} + \lambda_{T(i)} + \mu_i)S_i,\\
\frac{dU_i}{dt} &= \lambda_{H(i)}S_i - (\lambda_{T(i)} + \epsilon_i + \delta_{H(i)} + \mu_{(i)})U_i,\\
\frac{dD_i}{dt} &= \epsilon_{(i)}U_{i(i)} + d_{(i)}A_i - (\lambda_{T(i)} + \tau_{H(i)} + \mu_{(i)})D_i,\\
\frac{dA_i}{dt} &= D_i\tau_{H(i)} + (C_{LHi} + C_{THi})\tau_{C(i)} - (\mu_{(i)} + d_{(i)})A_i,\\
\frac{dE_i}{dt} &= \lambda_{T(i)}S_i + \theta_{(i)}R_i - (\alpha_{1(i)} + \lambda_{H(i)} + \mu_{(i)})E_i,\\
\frac{dI_i}{dt} &= \alpha_{1(i)}E_i - (\lambda_{H(i)} + \tau_{T(i)} + \delta_{T(i)} + \mu_{(i)})I_i,\\
\frac{dR_i}{dt} &= \tau_{T(i)}I_i - (\theta_{(i)} + \mu_{(i)})R_i,\\
\frac{dC_{LU(i)}}{dt} &= \lambda_{T(i)}U_i + \lambda_{H(i)}E_i - (\epsilon_{(i)} + \delta_{C1(i)} + \mu_{(i)})C_{LU(i)},\\
\frac{dC_{LH(i)}}{dt} &= \epsilon_{(i)}C_{LU(i)} + \lambda_{T(i)}D_i - (\tau_{C(i)} + \alpha_{2(i)} + \delta_{C2(i)}\\
&\quad + \mu_{(i)})C_{LH(i)},\\
\frac{dC_{TH(i)}}{dt} &= \alpha_{2(i)}C_{LHi} + \lambda_{H(i)}I_i - (\tau_{C(i)} + \delta_{C3(i)}\\
&\quad + \mu_{(i)})C_{TH(i)}
\end{aligned} \tag{3}$$

2.2. Model Analysis

This section investigates the positivity and boundedness of the solution. It is crucial for the formulated epidemiological model to be biologically reasonable [14].

2.2.1. Positivity

For realistic modeling of human population, all the state variables must be positive and the solutions to the model system with positive initial conditions should remain positive. This theorem is arrived at:

Theorem 2.1. For the given initial conditions of the model (3), the solutions of our model system remains positive for all $t > 0$.

Proof. Susceptible population: Taking the equation for the susceptible and assuming there is no disease,

$$\begin{aligned}
&\frac{dS_i}{dt} = \pi_{(i)} - (\lambda_{H(i)} + \lambda_{T(i)} + \mu_i)S_i \geq -\phi_s S_i\\
&\quad \implies \frac{dS_i}{dt} \geq -\phi_s S_i\\
&\frac{dS_i}{S_i} \geq -\phi_s dt \implies \ln|S_i| \geq -\phi_s t + c_1
\end{aligned}$$

for constant c_1 and $\phi_s = \mu_i$. Taking the exponential for both sides,

$$\begin{aligned}
e^{\ln|S_i|} &\geq e^{-\phi_s t + c_1} = Ke^{-\phi_s t}\\
S_i(t) &\geq Ke^{-\phi_s t}
\end{aligned}$$

where $K = e^{c_1}$ is a constant. Substituting the initial condition $S_i(0) = S_{i0}$, then

$$\begin{aligned}
S_i(0) &\geq Ke^{-\phi_s(0)} = S_{i0}\\
&\implies S_i(t) \geq S_{i0}e^{-\phi_s t}
\end{aligned}$$

Hence $K = S_{i0}$. The exponential part is always positive and $S_{i0} \geq 0$, hence $S_i(t)$ is always positive, meaning;

$$S_i(t) \geq 0$$

In the same way, all our states are *positive*,

$$
\begin{aligned}
U_i(t) \geq U_{i0}e^{-\phi_u t}, D_i(t) \geq D_{i0}e^{-\phi_d t}, A_i(t) \geq A_{i0}e^{-\phi_a t},\\
E_i(t) \geq E_{i0}e^{-\phi_e t}, I_i(t) \geq I_{i0}e^{-\phi_I t}, R_i(t) \geq R_{i0}e^{-\phi_r},\\
C_{LU(i)}(t) \geq C_{LU(i0)}e^{-\phi_{clu} t}, C_{LH(i)}(t) \geq C_{LH(i0)}e^{-\phi_{clh} t},\\
C_{TH(i)}(t) \geq C_{TH(i0)}e^{-\phi_{cth} t},
\end{aligned}
$$

given the initial conditions,

$$S_{i0}, U_{i0}, D_{i0}, A_{i0}, E_{i0}, I_{i0}, R_{i0}, C_{LUi0}, C_{LHi0}, C_{THi0} \tag{4}$$

2.2.2. Boundedness

Boundedness ensures population sizes within each compartment cannot grow indefinitely or exceed reasonable and feasible range. This arrives at,

Theorem 2.2. The solutions of the model system (3) with initial conditions given are bounded in a positive region, Ω

Proof.

$$
\begin{aligned}
\frac{dN_i}{dt} &= \frac{dS_i}{dt} + \frac{dU_i}{dt} + \frac{dD_i}{dt} + \frac{dA_i}{dt} + \frac{dE_i}{dt} + \frac{dI_i}{dt} + \frac{dR_i}{dt} + \frac{dC_{LUi}}{dt} + \frac{dC_{LHi}}{dt} + \frac{dC_{THi}}{dt}\\
\frac{dN}{dt} &= \pi_{(i)} - (S_i + U_i + D_i + A_i + E_i + I_i + R_i + C_{LUi} + C_{LHi} + C_{THi})\mu_i - \delta_{T(i)}I_i - \delta_{C1(i)}C_{LU(i)}\\
&\quad - \delta_{C2(i)}C_{LH(i)} - \delta_{C3(i)}C_{TH(i)}\\
\frac{dN_i}{dt} &= \pi_{(i)} - N_i\mu_i - \delta_{T(i)}I_i - \delta_{C1(i)}C_{LU(i)} - \delta_{C2(i)}C_{LH(i)} - \delta_{C3(i)}C_{TH(i)}
\end{aligned}
$$

Asumming there is no disease in the system,

$$\frac{dN_i}{dt} \leq \pi_{(i)} - N_i\mu_i.$$

Solving the above inequality using the integrating factor method and applying the initial condition, $N_i(0) = N_{i0}$,

$$N_i(t) \leq \frac{\pi_{(i)}}{\mu_i} + (N_{i0} - \frac{\pi_{(i)}}{\mu_i})e^{-\mu_i t}$$

If $N_{i0} > \frac{\pi_{(i)}}{\mu_i}$,, the right-hand side (RHS) experiences the largest possible value of N_{i0}. That is, $N_i(t) \leq N_{i0}$ for all $t > 0$.

If $N_{i0} < \frac{\pi_{(i)}}{\mu_i}$, so that the largest possible value of the RHS approaches $\frac{\pi_{(i)}}{\mu_i}$ as time t goes to infinity N_{i0}. That is, $N_i(t) \leq N_{i0}$ for all $t > 0$.

Hence $N_i(t) \leq \max\{N_{i0}, \frac{\pi_{(i)}}{\mu_i}\}\ \forall\ t > 0$ thus Ω

2.3. HIV Submodel Analysis

In this section, the model system 3 is analyzed by considering that TB is not present in the population. Thus, by substituting $E_i = I_i = T = C_{LU(i)} = C_{LH(i)} = C_{TH(i)} = 0$, the HIV sub-model is obtained as,

$$
\begin{aligned}
\frac{dS_i}{dt} &= \pi_{(i)} - (\lambda_{H(i)} + \lambda_{T(i)} + \mu_i)S_i,\\
\frac{dU_i}{dt} &= \lambda_{H(i)}S_i - (\lambda_{T(i)} + \epsilon_i + \delta_{H(i)} + \mu_{(i)})U_i,\\
\frac{dD_i}{dt} &= \epsilon_{(i)}U_{i(i)} + d_{(i)}A_i - (\lambda_{T(i)} + \tau_{H(i)} + \mu_{(i)})D_i,\\
\frac{dA_i}{dt} &= D_i\tau_{H(i)} + (C_{LHi} + C_{THi})\tau_{C(i)} - (\mu_{(i)} + d_{(i)})A_i.
\end{aligned} \tag{5}
$$

2.3.1. HIV-Free Equilibrium, $\hat{E_{H0}}$

The HIV-Free Equilibrium is obtained by setting the system of differential equations to zero and setting all infected classes to zero. The E_{H0},

$$\hat{E_{H0}} = \left(\frac{\pi_i}{\mu_i}, 0, 0, 0\right).$$

2.3.2. Endemic Equilibrium, $\hat{E_H}$

The endemic equilibrium is obtained by setting the system of differential equations to zero and solving for each variable. The EE,

$$\hat{E_H} = (\hat{S}_i, \hat{U}_i, \hat{D}_i, \hat{A}_i)$$

where,

$$\begin{aligned}
\hat{S}_i &= \frac{\pi_i}{(\lambda_{H(i)} + \lambda_{T(i)} + \mu_i)}, \\
\hat{U}_i &= \frac{\lambda_{H(i)}\pi_i}{h_1}, \\
\hat{D}_i &= \frac{\epsilon_i \hat{U}_i + d_i \hat{A}_i}{(\lambda_{T(i)} + \tau_{H(i)} + \mu_i)}, \\
\hat{A}_i &= \frac{\tau_{H(i)}\epsilon_i \lambda_{H(i)}\pi_i}{(\mu_i + d_i)(\lambda_{T(i)} + \tau_{H(i)} + \mu_i)h_1},
\end{aligned}$$

where $h_1 = (\lambda_{T(i)} + \epsilon_i + \delta_{H(i)} + \mu_i)(\lambda_{H(i)} + \lambda_{T(i)} + \mu_i)$.

2.3.3. Reproduction Number, R_0^H

Using the method by [15], the basic reproduction number was computed using the next generation matrix method. The disease infected classes that were considered are U_i, D_i, A_i to compute for R_0^H. The matrix $\mathcal{F}$ of new infections and matrix $\mathcal{V}$ showing the transfer of infections from one compartment to the other are generated.

$$\mathcal{F} = \begin{bmatrix} \lambda_{H(i)} S_i \\ 0 \\ 0 \end{bmatrix},$$

$$\mathcal{V} = \begin{bmatrix} (\lambda_{T(i)} + \epsilon_i + \delta_{H(i)} + \mu_i)U_i \\ -\epsilon_i U_i - d_i A_i + (\lambda_{T(i)} + \tau_{H(i)} + \mu_i)D_i \\ -\tau_{H(i)} D_i + (C_{LH(i)} + C_{TH(i)})\tau_{C(i)} + (\mu_i + d_i)A_i \end{bmatrix}.$$

Computing the derivatives with respect to U_i, D_i, A_i and substituting for DFE to get the Jacobian matrices F and V,

$$F = \begin{bmatrix} \beta_{H(i)} & \beta_{H(i)} & \eta_i \beta_{H(i)} \\ 0 & 0 & 0 \\ 0 & 0 & 0 \end{bmatrix},$$

$$V = \begin{bmatrix} \delta_{H(i)} + \mu_i + \epsilon_i & 0 & 0 \\ -\epsilon_i & \tau_{H(i)} + \mu_i & -d_i \\ 0 & -\tau_{H(i)} & d_i + \mu_i \end{bmatrix}.$$

The next generation matrix is computed and given by FV^{-1},

$$\begin{bmatrix} \frac{\beta_{H(i)} h_1}{h_2\left(\delta_{H(i)} + \mu_i + \epsilon_i\right)} & \frac{\beta_{H(i)}\left(d_i + \eta_i \tau_{H(i)} + \mu_i\right)}{h_2} & \frac{\beta_{H(i)}\left(d_i + \eta_i \mu_i + \eta_i \tau_{H(i)}\right)}{h_2} \\ 0 & 0 & 0 \\ 0 & 0 & 0 \end{bmatrix},$$

where $h_2 = \Big((d_i + \mu_i)(\mu_i + \epsilon_i) + \tau_{H(i)}(\mu_i + \eta_i \epsilon_i)\Big), h_3 = \mu_i\left(d_i + \tau_{H(i)} + \mu_i\right)$. Computing the eigenvalues of the matrix FV^-1 to obtain R_0,

$$R_0^H = \frac{\beta_{H(i)}\left((d_i + \mu_i)(\mu_i + \epsilon_i) + \tau_{H(i)}(\mu_i + \eta_i \epsilon_i)\right)}{\mu_i\left(d_i + \tau_{H(i)} + \mu_i\right)\left(\delta_{H(i)} + \mu_i + \epsilon_i\right)}.$$

2.3.4. Stability Analysis of HIV-Free Equilibrium

The local stability analysis of the HIV-free equilibrium point (E_{H0}) of the model is determined by finding the Jacobian matrix and its eigenvalues [16]. An equilibrium point is locally asymptotically stable if all the eigenvalues of the Jacobian matrix at that point are negative. The general Jacobian matrix of model, $J_{E_{H0}}$, is written as:

$$\begin{bmatrix} -\mu_i & -\beta_{H(i)} & -\beta_{H(i)} & -\eta_i\beta_{H(i)} \\ 0 & \beta_{H(i)} - (\epsilon_i + \delta_{H(i)} + \mu_i) & \beta_{H(i)} & \eta_i\beta_{H(i)} \\ 0 & \epsilon_i & -(\tau_{H(i)} + \mu_i) & d_i \\ 0 & 0 & \tau_{H(i)} & -(d_i + \mu_i) \end{bmatrix}.$$

By inspection of J_{E_0}, the first eigenvalue is on row 1, column 1, $\lambda_1 = -\mu_i$ which is negative. The row and column are eliminated with which the eigenvalue is contained to get the reduced matrix to be,

$$\begin{bmatrix} \beta_{H(i)} - (\epsilon_i + \delta_{H(i)} + \mu_i) & \beta_{H(i)} & \eta_i\beta_{H(i)} \\ \epsilon_i & -(\tau_{H(i)} + \mu_i) & d_i \\ 0 & \tau_{H(i)} & -(d_i + \mu_i) \end{bmatrix}.$$

The Routh-Hurwitz criterion

A 3rd-degree polynomial,

$$p(s) = s^3 + a_1 s^2 + a_2 s + a_3, \tag{6}$$

is stable if and only if $a_1, a_2, a_3 > 0$ and $a_1 a_2 > a_3$.

Rourth-Hurtwiz criterion is used to determine when the eigenvalues are negative [17]. The characteristic polynomial are determined using the trace, sum of diagonal minors and the determinant. The characteristic polynomial $P(s)$ is given by,

$$\begin{aligned} P(s) = s^3 - [\beta_{H(i)} - d_i - \delta_{H(i)} - \tau_{H(i)} - 3\mu_i - \epsilon_i]s^2 - [\beta_{H(i)}\left(d_i + \tau_{H(i)} + 2\mu_i + \epsilon_i\right) - \delta_{H(i)}(d_i + \tau_{H(i)} \\ +2\mu_i) - 2\mu_i(d_i + \epsilon_i) - d_i\epsilon_i - \tau_{H(i)}(2\mu_i + \epsilon_i) - 3\mu_i^2]s - [\beta_{H(i)}[(d_i + \mu_i)(\mu_i + \epsilon_i) + \tau_{H(i)}(\mu_i \\ + \eta_i\epsilon_i)] - \mu_i\left(d_i + \tau_{H(i)} + \mu_i\right)\left(\delta_{H(i)} + \mu_i + \epsilon_i\right)]. \end{aligned} \tag{7}$$

Hence stability is achieved by, $a_1, a_2, a_3 > 0$ and $a_1 a_2 > a_3$ where,

$$\begin{aligned} a_1 &= d_i + \delta_{H(i)} + \tau_{H(i)} + 3\mu_i + \epsilon_i - \beta_{H(i)}, \\ a_2 &= \beta_{H(i)}\left(d_i + \tau_{H(i)} + 2\mu_i + \epsilon_i\right) - \delta_{H(i)}[d_i + \tau_{H(i)} + 2\mu_i] - 2\mu_i(d_i + \epsilon_i) - d_i\epsilon_i - \tau_{H(i)}(2\mu_i + \epsilon_i) - 3\mu_i^2, \\ a_3 &= \beta_{H(i)}\left((d_i + \mu_i)(\mu_i + \epsilon_i) + \tau_{H(i)}(\mu_i + \eta_i\epsilon_i)\right) - \mu_i\left(d_i + \tau_{H(i)} + \mu_i\right)\left(\delta_{H(i)} + \mu_i + \epsilon_i\right). \end{aligned}$$

2.3.5. Global Stability of the HIV-Free Equilibrium

The method illustrated in [18, 19] is used to investigate the global asymptotic stability (GAS) of DFE point of the HIV model, E_0^H. Firstly, the model 5 must be written in the pseudotriangular form:

$$\dot{X}_1 = A_1(X_1 - X_1^*) + A_2X_2, \tag{8}$$

$$\dot{X}_2 = A_3X_2, \tag{9}$$

where $X_1 = (S_i)$, represents the number of uninfected individuals and $X_2 = (U_i, D_i, A_i)$, denotes the number of infected individuals. Let X^* be the HIV-free equilibrium. From X_1,

$$A_1 = \begin{bmatrix} -\mu_i \end{bmatrix}, A_2 = \begin{bmatrix} -\beta_{H(i)} & -\beta_{H(i)} & -\eta_i\beta_{H(i)} \end{bmatrix}.$$

We can easily see that the eigenvalue of matrix A_1 is both real and negative ($-\mu_i < 0$). This shows that the subsystem $\dot{X}_1 = A_1(X_1 - X_1^*) + A_2X_2$, is globally asymptotically stable at the HIV free equilibrium $X_1^* = \left(\frac{\pi_i}{\mu_i}\right)$. Additionally, from subsystem$X_2 = A_3X_2$, we obtain the following matrix A_3,

$$\begin{bmatrix} \beta_{H(i)} - (\delta_{H(i)} + \mu_i + \epsilon_i) & \beta_{H(i)} & \eta_i\beta_{H(i)} \\ \epsilon_i & -(\tau_{H(i)} + \mu_i) & d_i \\ 0 & \tau_{H(i)} & -(d_i + \mu_i) \end{bmatrix}. \tag{10}$$

Notice that all the off-diagonal entries of A_3 are nonnegative (equal to or greater than zero), showing that A_3 is a Metzler matrix. To show the global stability of the HIV-free equilibrium E_{T0}, we need to show that the square matrix A_3 in (10) is Metzler stable. We therefore need to prove the following;

Lemma 2.1. Let M be a square Metzler matrix that is block decomposed:

$$M = \begin{bmatrix} A & B \\ C & D \end{bmatrix} \tag{11}$$

,

where A and D are square matrices. The matrix M is Metzler stable if and only if A and $D - CA^{-1}B$ are Metzler stable.

Proof. Matrix M in our case is A_3. We therefore let,

$$\begin{aligned} A &= \begin{bmatrix} \beta_{H(i)} - (\delta_{H(i)} + \mu_i + \epsilon_i) & \beta_{H(i)} \\ \epsilon_i & -\tau_{H(i)} - \mu_i \end{bmatrix}, \\ B &= \begin{bmatrix} \eta_i \beta_{H(i)} \\ d_i \end{bmatrix}, C = \begin{bmatrix} 0 & \tau_{H(i)} \end{bmatrix} \ \& \ D = \begin{bmatrix} -(d_i + \mu_i) \end{bmatrix}. \end{aligned} \tag{12}$$

Clearly, A is Metzler stable if $\dfrac{\beta_{H(i)}}{(\delta_{H(i)} + \mu_i + \epsilon_i)} < 1$. Then,

$$D - CA^{-1}B = \left[\frac{\beta_{H(i)} h_2 - h_3 \left(\delta_{H(i)} + \mu_i + \epsilon_i\right)}{\left(\tau_{H(i)} + \mu_i\right)\left(\delta_{H(i)} + \mu_i + \epsilon_i\right) - \beta_{H(i)}\left(\tau_{H(i)} + \mu_i + \epsilon_i\right)} \right] \tag{13}$$

From (13), $D - CA^{-1}B$ is Metzler stable when the main diagonal element is negative. Simplifying the element,

$$\begin{aligned} \frac{\beta_{H(i)} \left[(d_i + \mu_i)(\mu_i + \epsilon_i) + \tau_{H(i)}(\mu_i + \eta_i \epsilon_i)\right]}{\mu_i \left(d_i + \tau_{H(i)} + \mu_i\right)\left(\delta_{H(i)} + \mu_i + \epsilon_i\right)} &< 1, \\ R_0^H &< 1. \end{aligned}$$

Hence E_0^H is $G.A.S$ when $R_0^H < 1$.

Thus the HIV free Equilibrium point $E_O^T H$ is globally asymptotically stable. Epidemiologically, the above result implies that when there is no HIV infection, different human populations under consideration will stabilize at the E_O^H. However, if there exists a HIV infection infection, then an appropriate control e.g. HIV ART treatment would be necessary to control the disease and restore the system to the stable HIV-free equilibrium.

2.4. TB Submodel Analysis

In this section, the model system 3 is analyzed by considering that HIV is not present in the population. Thus, by substituting $U_i = D_i = A_i = C_{LU(i)} = C_{LH(i)} = C_{TH(i)} = 0$, the TB sub-model is obtained as,

$$\begin{aligned} \frac{dS_i}{dt} &= \pi_{(i)} - (\lambda_{H(i)} + \lambda_{T(i)} + \mu_i) S_i, \\ \frac{dE_i}{dt} &= \lambda_{T(i)} S_i + \theta_{(i)} R_i - (\alpha_{1(i)} + \lambda_{H(i)} + \mu_{(i)}) E_i, \\ \frac{dI_i}{dt} &= \alpha_{1(i)} E_i - (\lambda_{H(i)} + \tau_{T(i)} + \delta_{T(i)} + \mu_{(i)}) I_i, \\ \frac{dR_i}{dt} &= \tau_{T(i)} I_i - (\theta_{(i)} + \mu_{(i)}) R_i. \end{aligned} \tag{14}$$

2.4.1. TB-Free Equilibrium, E_{T0}

The TB-Free Equilibrium is obtained by setting the system of differential equations to zero and setting all infected classes to zero. The E_{T0},

$$E_{T0} = \left(\frac{\pi_i}{\mu_i}, 0, 0, 0 \right).$$

2.4.2. Endemic Equilibrium, E_T

The endemic equilibrium is obtained by setting the system of differential equations to zero and solving for each variable. The EE,

$$\hat{E_T} = (\hat{S_i}, \hat{E_i}, \hat{I_i}, \hat{R_i})$$

where,

$$\hat{S_i} = \frac{\pi_i}{(\lambda_{H(i)} + \lambda_{T(i)} + \mu_i)},$$

$$\hat{E_i} = \frac{\hat{S_i}}{(\alpha_{1(i)} + \lambda_{H(i)} + \mu_i)} \left(\alpha_T + \frac{\theta_i \tau_{T(i)} \alpha_{1(i)} \lambda_{T(i)}}{h_4} \right),$$

$$\hat{I_i} = \frac{\alpha_{1(i)} \lambda_{T(i)} \pi_i (\theta_i + \mu_i)}{(\lambda_{H(i)} + \lambda_{T(i)} + \mu_i) h_4},$$

$$\hat{R}_i = \frac{\tau_{T(i)}\alpha_{1(i)}\lambda_{T(i)}\pi_i}{(\lambda_{H(i)} + \lambda_{T(i)} + \mu_i)h_4},$$

where is $h_4 = ((\theta_i + \mu_i)(\alpha_{1(i)} + \lambda_{H(i)} + \mu_i)(\lambda_{H(i)} + \tau_{T(i)} + \delta_{T(i)} + \mu_i) - \alpha_{1(i)}\theta_i\tau_{H(i)})$.

2.4.3. Reproduction Number, R_0^T

Using the method by [15], the basic reproduction number was computed using the next generation matrix method. The disease infected classes that were considered are E_i, I_i to compute for R_0^T. The matrix $\mathcal{F}$ of new infections and matrix $\mathcal{V}$ showing the transfer of infections from one compartment to the other are generated.

$$\mathcal{F} = \begin{bmatrix} \lambda_{T(i)}S_i + \theta_i R_i \\ 0 \end{bmatrix},$$

$$\mathcal{V} = \begin{bmatrix} (\alpha_{1(i)} + \lambda_{H(i)} + \mu_i)E_i \\ -\alpha_{1(i)}E_i + (\lambda_{H(i)} + \tau_{T(i)} + \delta_{T(i)} + \mu_i)I_i \end{bmatrix}.$$

Computing the derivatives with respect to E_i, I_i and substituting for DFE to get the Jacobian matrices F and V,

$$F = \begin{bmatrix} 0 & \beta_{T(i)} \\ 0 & 0 \end{bmatrix},$$

$$V = \begin{bmatrix} \alpha_{1(i)} + \mu_i & 0 \\ -\alpha_{1(i)} & \tau_{T(i)} + \delta_{T(i)} + \mu_i \end{bmatrix}.$$

Computing the next generation matrix given by,

$$FV^{-1} = \begin{bmatrix} \frac{\alpha_{1(i)}\beta_{T(i)}}{h_5} & \frac{\beta_{T(i)}}{\tau_{T(i)}+\delta_{T(i)}+\mu_i} \\ 0 & 0 \end{bmatrix}$$

where $h_5 = \alpha_{1(i)}\delta_{T(i)} + \mu_i^2 + \alpha_{1(i)}\mu_i + \delta_{T(i)}\mu_i + \alpha_{1(i)}\tau_{T(i)} + \mu_i\tau_{T(i)}$. Computing the eigenvalues of the matrix $FV^{-}1$ to obtain R_0,

$$R_0^T = \frac{\alpha_{1(i)}\beta_{T(i)}}{(\alpha_{1(i)} + \mu_i)(\tau_{T(i)} + \delta_{T(i)} + \mu_i)}.$$

2.4.4. Local Stability of TB-Free Equilibrium

The general Jacobian matrix, $J_{E_{T0}}$ of model after substituting E_{T0} is written as:

$$\begin{bmatrix} -\mu_i & 0 & -\beta_{T(i)} & 0 \\ 0 & -(\alpha_{1(i)} + \mu_i) & 0 & \theta_i \\ 0 & \alpha_{1(i)} & -(\delta_{T(i)} + \mu_i + \tau_{T(i)}) & 0 \\ 0 & 0 & \tau_{T(i)} & -(\theta_i + \mu_i) \end{bmatrix}.$$

By inspection on row 1 and column 1, a negative eigenvalue $\lambda_1 = -\mu_i$ is gotten. The matrix reduces to;

$$J_{E_0} = \begin{bmatrix} -(\alpha_{1(i)} + \mu_i) & 0 & \theta_i \\ \alpha_{1(i)} & -(\delta_{T(i)} + \mu_i + \tau_{T(i)}) & 0 \\ 0 & \tau_{T(i)} & -(\theta_i + \mu_i) \end{bmatrix}. \tag{15}$$

The Routh-Hurwitz criterion

The characteristic polynomial of (15) is computed and (6) criteria is used as applied in HIV sub-model.

$$\begin{aligned} P(s) = s^3 &+ [(\alpha_{1(i)} + \delta_{T(i)} + \tau_{T(i)} + \theta_i + 3\mu_i)]s^2 - [(\delta_{T(i)} \\ &+ \mu_i + \tau_{T(i)})(\theta_i + \mu_i) + (\alpha_{1(i)} + \mu_i)(\theta_i + \mu_i) \\ &+ (\alpha_{1(i)} + \mu_i)(\delta_{T(i)} + \mu_i + \tau_{T(i)})]s + [\mu_i^2(\alpha_{1(i)} + \delta_{T(i)} \\ &+ \theta_i + \tau_{T(i)} + \mu_i) + \theta_i\mu_i(\alpha_{1(i)} + \delta_{T(i)} + \tau_{T(i)}) \\ &+ \alpha_{1(i)}\mu_i(\delta_{T(i)} + \tau_{T(i)} + \frac{\delta_{T(i)}\theta_i}{\mu_i})]. \end{aligned}$$

Hence stability is achieved by,

1. $(\alpha_{1(i)} + \delta_{T(i)} + \tau_{T(i)} + \theta_i + 3\mu_i) > 0$,
2. $[(\delta_{T(i)} + \mu_i + \tau_{T(i)})(\theta_i + \mu_i) + (\alpha_{1(i)} + \mu_i)(\theta_i + \mu_i) + (\alpha_{1(i)} + \mu_i)(\delta_{T(i)} + \mu_i + \tau_{T(i)})] > 0$,
3. $[\mu_i^2(\alpha_{1(i)} + \delta_{T(i)} + \theta_i + \tau_{T(i)} + \mu_i) + \theta_i\mu_i(\alpha_{1(i)} + \delta_{T(i)} + \tau_{T(i)}) + \alpha_{1(i)}\mu_i(\delta_{T(i)} + \tau_{T(i)} + \frac{\delta_{T(i)}\theta_i}{\mu_i})] > 0$,
4. $(\alpha_{1(i)} + \delta_{T(i)} + \tau_{T(i)} + \theta_i + 3\mu_i)[(\delta_{T(i)} + \mu_i + \tau_{T(i)})(\theta_i + \mu_i) + (\alpha_{1(i)} + \mu_i)(\theta_i + \mu_i) + (\alpha_{1(i)} + \mu_i)(\delta_{T(i)} + \mu_i + \tau_{T(i)})] > [\mu_i^2(\alpha_{1(i)} + \delta_{T(i)} + \theta_i + \tau_{T(i)} + \mu_i) + \theta_i\mu_i(\alpha_{1(i)} + \delta_{T(i)} + \tau_{T(i)}) + \alpha_{1(i)}\mu_i(\delta_{T(i)} + \tau_{T(i)} + \frac{\delta_{T(i)}\theta_i}{\mu_i})]$.

2.4.5. Global Stability of the TB-Free Equilibrium

The method illustrated in [18, 19] is used to investigate the global asymptotic stability (GAS) of DFE point of the TB model, E_0^T. Firstly, the model 14 must be written in the pseudotriangular form:

$$\dot{X}_1 = A_1(X_1 - X_1^*) + A_2X_2, \tag{16}$$

$$\dot{X}_2 = A_3X_2, \tag{17}$$

where $X_1 = (S_i, R_i)$, represents the number of uninfected individuals and $X_2 = (E_i, I_i)$, denotes the number of infected individuals. Let X^* be the TB-free equilibrium. From X_1,

$$A_1 = \begin{bmatrix} -\mu_i & 0 \\ 0 & -(\theta_i + \mu_i) \end{bmatrix}, A_2 = \begin{bmatrix} 0 & -\beta_{T(i)} \\ 0 & \tau_{T(i)} \end{bmatrix}.$$

We can easily see that the eigenvalues of matrix $A1$ are both real and negative $(-\mu_i < 0, -(\theta_i + \mu_i) < 0)$. This shows that the subsystem $\dot{X}_1 = A_1(X_1 - X_1^*) + A_2X_2$, is globally asymptotically stable at the TB free equilibrium $X_1^* = \left(\frac{\pi_i}{\mu_i}, 0\right)$. Additionally, from subsystem $X_2 = A_3X_2$, we obtain the following matrix,

$$A_3 = \begin{bmatrix} -(\alpha_{1(i)} + \mu_i) & \beta_{T(i)} \\ \alpha_{1(i)} & -(\mu_i + \delta_{T(i)} + \tau_{T(i)}) \end{bmatrix}. \tag{18}$$

Notice that all the off-diagonal entries of A_3 are nonnegative (equal to or greater than zero), showing that A_3 is a Metzler matrix. To show the global stability of the TB-free equilibrium E_{T0}, we need to show that the square matrix A_3 in (18) is Metzler stable. We therefore need to prove the lemma outlined at (11).

Proof. Matrix M in our case is A_3. We therefore let,

$$\begin{aligned} A &= \left[-(\alpha_{1(i)} + \mu_i)\right], B = \left[\beta_{T(i)}\right], \\ C &= \left[\alpha_{1(i)}\right] \ \& \ D = \left[-(\mu_i + \delta_{T(i)} + \tau_{T(i)})\right]. \end{aligned} \tag{19}$$

Clearly, A is Metzler stable. Then,

$$D - CA^{-1}B = \left[\left(-(\mu_i + \delta_{T(i)} + \tau_{T(i)}) + \frac{\alpha_{1(i)}\beta_{T(i)}}{(\alpha_{1(i)} + \mu_i)}\right)\right]. \tag{20}$$

From (20), $D - CA^{-1}B$ is Metzler stable when the main diagonal element is strictly negative. This can be achieved by reorganizing the diagonal element as follows,

$$\begin{aligned} \left(-(\mu_i + \delta_{T(i)} + \tau_{T(i)}) + \frac{\alpha_{1(i)}\beta_{T(i)}}{(\alpha_{1(i)} + \mu_i)}\right) &< 0, \\ \frac{\alpha_{1(i)}\beta_{T(i)}}{(\alpha_{1(i)} + \mu_i)} &< (\mu_i + \delta_{T(i)} + \tau_{T(i)}), \\ \frac{\alpha_{1(i)}\beta_{T(i)}}{(\alpha_{1(i)} + \mu_i)(\mu_i + \delta_{T(i)} + \tau_{T(i)})} &< 1, \\ R_0^T &< 1. \end{aligned}$$

Hence E_0^T is $G.A.S$ when $R_0^T \& < 1$.

Thus the TB free Equilibrium point E_O^T is globally asymptotically stable. Epidemiologically, the above result implies that when there is no TB infection, different human populations under consideration will stabilize at the E_O^T. However, if there exists a TB infection, then an appropriate control e.g. TB treatment would be necessary to control the disease and restore the system to the stable TB-free equilibrium.

2.5. Full Model Analysis

The whole system (3) is considered for full model analysis.

2.5.1. Disease-Free Equilibrium

The disease free equilibrium is obtained by setting the system of differential equations to zero and setting all infected classes to zero to get,

$$E_0 = \left(\frac{\pi_i}{\mu_i}, 0, 0, 0, 0, 0, 0, 0, 0, 0\right).$$

2.5.2. Endemic Equilibrium, $\hat{E}_i$

The EE equilibrium is obtained by setting the system of differential equations 3 to zero and solving for each variable. The $\hat{E}_i$,

$$\hat{E}_i = (\hat{S}_i, \hat{U}_i, \hat{D}_i, \hat{A}_i, \hat{E}_i, \hat{I}_i, \hat{R}_i, \hat{C_{LU(i)}}, \hat{C_{LH(i)}}, \hat{C_{TH(i)}})$$

where,

$$\hat{S}_i = \frac{\pi_i}{(\lambda_{H(i)} + \lambda_{T(i)} + \mu_i)}, \hat{U}_i = \frac{\lambda_{H(i)}\pi_i}{h_6},$$

$$\hat{D}_i = \frac{\epsilon_i \lambda_{H(i)}\pi_i}{(\lambda_{T(i)} + \tau_{H(i)} + \mu_i)h_6},$$

$$\hat{A}_i = \frac{\tau_{H(i)}\epsilon_i \lambda_{H(i)}\pi_i}{\mu_i(\lambda_{T(i)} + \tau_{H(i)} + \mu_i)h_6} + \tau_{C(i)}(\hat{C_{LH}} + \hat{C_{TH}}),$$

$$\hat{E}_i = \frac{1}{(\alpha_{1(i)} + \lambda_{H(i)} + \mu_i)}\left(\alpha_T \hat{S}_i + \frac{\theta_i \tau_{T(i)}\alpha_{1(i)}\lambda_{T(i)}}{h_4}\hat{S}_i\right),$$

$$\hat{I}_i = \frac{\alpha_{1(i)}\lambda_{T(i)}\pi_i(\theta_i + \mu_i)}{(\lambda_{H(i)} + \lambda_{T(i)} + \mu_i)h_4}, \hat{T} = \frac{\tau_{T(i)}\alpha_{1(i)}\lambda_{T(i)}\pi_i}{(\lambda_{H(i)} + \lambda_{T(i)} + \mu_i)h_4},$$

$$\hat{C_{LU(i)}} = \frac{1}{(\epsilon_i + \delta_{c1} + \mu_i)}\left(\frac{\lambda_{T(i)}\lambda_{H(i)}\pi_i}{h_6} + \lambda_{H(i)}\hat{E}_i\right),$$

$$\hat{C_{LH(i)}} = \frac{1}{h_7}\left(\epsilon_i \hat{C_{LU(i)}} + \frac{\lambda_{T(i)}\epsilon_i\lambda_{H(i)}\pi_i}{h_6}\right),$$

$$\hat{C_{TH(i)}} = \frac{1}{(\tau + \delta_{C1(i)} + \mu_i)}\left(\alpha_{2(i)}\hat{C_{LH(i)}} + \frac{\lambda_{H(i)}\alpha_{1(i)}\lambda_{T(i)}(\theta_i + \mu_i)}{h_4}\hat{S}_i\right),$$

where $h_4 = ((\theta_i+\mu_i)(\alpha_{1(i)}+\lambda_{H(i)}+\mu_i)(\lambda_{H(i)}+\tau_{T(i)}+\delta_{T(i)}+\mu_i)-\alpha_{1(i)}\theta_i\tau_{H(i)})$ and $h_6 = (\lambda_{T(i)}+\epsilon_i+\delta_{H(i)}+\mu_i)(\lambda_{H(i)}+\lambda_{T(i)}+\mu_i)$.

2.5.3. Basic Reproduction Number

Using the method by [15], the basic reproduction number was computed using the next generation matrix method. The infectious classes that were considered are $U_i, D_i, A_i, C_{LU(i)}, C_{LH(i)}, C_{TH(i)}, I_i$ to compute for R_0. The matrix $\mathcal{F}$ of new infections and matrix $\mathcal{V}$ showing the transfer of infections from one compartment to the other are generated.

$$\mathcal{F} = \begin{bmatrix} \lambda_{H(i)}S_i \\ 0 \\ 0 \\ \lambda_{T(i)}U_i + \lambda_{H(i)}E_i \\ 0 \\ 0 \\ \alpha_{1(i)}E_i \end{bmatrix}, \tag{21}$$

and

$$\mathcal{V} = \begin{bmatrix} (\lambda_{T(i)} + \epsilon_i + \delta_{H(i)} + \mu_i)U_i \\ -\epsilon_i U_i - d_i A_i + (\lambda_{T(i)} + \tau_{H(i)} + \mu_i)D_i \\ -\tau_{H(i)}D_i - (C_{LH(i)} + C_{TH(i)})\tau_{C(i)} + (\mu_i + d_i)A_i \\ (\epsilon_i + \delta_{c1} + \mu_i)C_{LU(i)} \\ -\epsilon_i C_{LU(i)} - \lambda_{T(i)}D_i + h_7 C_{LH(i)} \\ -\alpha_{2(i)}C_{LH(i)} - \lambda_{H(i)}I_i + (\tau + \delta_{C1(i)} + \mu_i)C_{TH(i)} \\ (\lambda_{H(i)} + \delta_{T(i)} + \tau_{T(i)} + \mu_i)I_i \end{bmatrix}, \tag{22}$$

where $h_7 = (\tau_{C(i)} + \alpha_{2(i)} + \delta_{C1(i)} + \mu_i)$ The derivatives with respect to $U_i, D_i, A_i, C_{LU(i)}, C_{LH(i)}, C_{TH(i)}, I_i$ are computed

and substituted for E_0 to get the Jacobian matrices F and V. Computing the next generation matrix given by,

$$FV^{-1} = \begin{bmatrix} g_1^* g_1 & g_2^* g_1 & g_3^* g_1 & g_2 & g_3 & g_4 & 0 \\ 0 & 0 & 0 & 0 & 0 & 0 & 0 \\ 0 & 0 & 0 & 0 & 0 & 0 & 0 \\ 0 & 0 & 0 & 0 & 0 & 0 & 0 \\ 0 & 0 & 0 & 0 & 0 & 0 & 0 \\ 0 & 0 & 0 & 0 & 0 & 0 & 0 \\ 0 & 0 & 0 & 0 & 0 & 0 & 0 \end{bmatrix}.$$

Where,

$$g_1 = \frac{\beta_{H(i)}}{\mu_i \left(d_i + \tau_{H(i)} + \mu_i\right)}, g_1^* = \frac{h_2}{\left(\delta_{H(i)} + \mu_i + \epsilon_i\right)}$$
$$g_2^* = (d_i + \eta_i \tau_{H(i)} + \mu_i),\ g_3^* = (d_i + \eta_i(\mu_i + \tau_{H(i)})),$$

$$g_4^* = \mu_i \left(d_i + \tau_{H(i)} + \mu_i\right) \left(\tau_{C(i)} + \delta_{\text{C3(i)}} + \mu_i\right),$$
$$g_5^* = (\alpha_{2(i)} + \tau_{C(i)} + \mu_i),$$
$$g_2 = \frac{g_4^* \left(g_5^* + \delta_{\text{C2(i)}}\right) + d_i \epsilon_i \tau_{C(i)} \left(g_5^* + \delta_{\text{C3(i)}}\right)}{\left(\delta_{\text{C1(i)}} + \mu_i + \epsilon_i\right) \left(\tau_{C(i)} + \delta_{\text{C3(i)}} + \mu_i\right) \left(g_5^* + \delta_{\text{C2(i)}}\right)} g_1 + \frac{\epsilon_i g_4^* + h_8 + \alpha_{2(i)} \mu_i \epsilon_i \left(d_i + \tau_{H(i)} + \mu_i\right)}{\left(\delta_{\text{C1(i)}} + \mu_i + \epsilon_i\right) \left(\tau_{C(i)} + \delta_{\text{C3(i)}} + \mu_i\right) \left(g_5^* + \delta_{\text{C2(i)}}\right)} g_1,$$
$$g_3 = \frac{\left(\alpha_{2(i)} + \tau_{C(i)} + \delta_{\text{C3(i)}} + \mu_i\right)}{\left(\alpha_{2(i)} + \tau_{C(i)} + \delta_{\text{C2(i)}} + \mu_i\right)} g_4,$$
$$g_4 = \frac{\left(\tau_{C(i)} \left(d_i + \eta_i \mu_i + \eta_i \tau_{H(i)}\right) + \mu_i \left(d_i + \tau_{H(i)} + \mu_i\right)\right)}{\left(\tau_{C(i)} + \delta_{\text{C3(i)}} + \mu_i\right)} g_1,$$
$$h_8 = \eta_i \epsilon_i \tau_{C(i)} \left(\tau_{H(i)} + \mu_i\right) \left(g_5^* + \delta_{\text{C3(i)}}\right).$$

Computing the eigenvalues of the matrix $FV^{-}1$ to obtain that the basic reproduction number of the co-infection model is the maximum of the absolute values of the eigenvalues of R_0^C which is given by,

$$R_0^C = \max\{R_0^H, R_0^T\}.$$

Thus, the following result has been stated arising from the theorem of [20].

2.5.4. Local Stability of Disease Free Equilibrium

The local stability analysis of the disease-free equilibrium point (DFE) of the model is determined by finding the Jacobian matrix and its eigenvalues [16]. An equilibrium point is locally asymptotically stable if all the eigenvalues of the Jacobian matrix at that point are negative. The general Jacobian matrix of model is written as:

$$\begin{bmatrix} -\mu_i & -\beta_{H(i)} & -\beta_{H(i)} & -\eta_i \beta_{H(i)} & 0 & -\beta_{T(i)} & 0 & -\beta_{H(i)} & -\beta_{H(i)} & -(\beta_{H(i)} + \beta_{T(i)}) \\ 0 & c_0 & \beta_{H(i)} & \eta_i \beta_{H(i)} & 0 & 0 & 0 & \beta_{H(i)} & \beta_{H(i)} & \beta_{H(i)} \\ 0 & \epsilon_i & -(\tau_{H(i)} + \mu_i) & d_i & 0 & 0 & 0 & 0 & 0 & 0 \\ 0 & 0 & \tau_{H(i)} & -(d_i + \mu_i) & 0 & 0 & 0 & 0 & \tau_{C(i)} & \tau_{C(i)} \\ 0 & 0 & 0 & 0 & -(\alpha_{1(i)} + \mu_i) & \beta_{T(i)} & \theta_i & 0 & 0 & \beta_{T(i)} \\ 0 & 0 & 0 & 0 & \alpha_{1(i)} & -c_5 & 0 & 0 & 0 & 0 \\ 0 & 0 & 0 & 0 & 0 & \tau_{T(i)} & -(\theta_i + \mu_i) & 0 & 0 & 0 \\ 0 & 0 & 0 & 0 & 0 & 0 & 0 & -c_1 & 0 & 0 \\ 0 & 0 & 0 & 0 & 0 & 0 & 0 & \epsilon_i & -c_2 & 0 \\ 0 & 0 & 0 & 0 & 0 & 0 & 0 & 0 & \alpha_{2(i)} & -c_3 \end{bmatrix}.$$

where $c_0 = \beta_{H(i)} - (\delta_{H(i)} + \mu_i + \epsilon_i), c_1 = (\delta_{\text{C1(i)}} + \mu_i + \epsilon_i), c_2 = (\alpha_{2(i)} + \tau_{C(i)} + \delta_{\text{C2(i)}} + \mu_i), c_3 = (\tau_{C(i)} + \delta_{\text{C3(i)}} + \mu_i)$ and $c_5 = (\mu_i + \delta_{T(i)} + \tau_{T(i)})$. Clearly $-\mu_i, -(d_i + \mu_i), -(\mu_i + \delta_{T(i)} + \tau_{T(i)}), -(\theta_i + \mu_i), -(\delta_{\text{C1(i)}} + \mu_i + \epsilon_i), -(\alpha_{2(i)} + \tau_{C(i)} + \delta_{\text{C2(i)}} + \mu_i)$ are the six negative eigenvalues of the jacobian matrix above. The matrix reduces to;

$$\begin{bmatrix} c_0 & \beta_{H(i)} & 0 & \beta_{H(i)} \\ \epsilon_i & -(\tau_{H(i)}+\mu_i) & 0 & 0 \\ 0 & 0 & -(\alpha_{1(i)}+\mu_i) & \beta_{T(i)} \\ 0 & 0 & 0 & -c_3 \end{bmatrix}.$$

The other four remaining eigenvalues of the matrix are the zeros of the polynomial,

$$P(s) = s^4 + A_1 s^3 + A_2 s^2 + A_3 s + A_4, \tag{23}$$

where,

$$\begin{aligned}
A_1 &= \alpha_{1(i)} + \tau_{C(i)} + \delta_{\text{C3(i)}} - \beta_{H(i)} + \delta_{H(i)} + \tau_{H(i)} + 4\mu_i + \epsilon_i, \\
A_2 &= \alpha_{1(i)}[\tau_{C(i)} + \delta_{\text{C3(i)}} - \beta_{H(i)} + \delta_{H(i)} + \tau_{H(i)} + 3\mu_i + \epsilon_i] - \beta_{H(i)}[\tau_{C(i)} + \delta_{\text{C3(i)}} + \tau_{H(i)} + 3\mu_i + \epsilon_i] \\
&\quad + \tau_{H(i)}\left(\tau_{C(i)} + \delta_{\text{C3(i)}} + \delta_{H(i)} + 3\mu_i + \epsilon_i\right) + \tau_{C(i)}\delta_{H(i)} + 3\mu_i\tau_{C(i)} + \epsilon_i\tau_{C(i)} + 3\mu_i\delta_{\text{C3(i)}} + \epsilon_i\delta_{\text{C3(i)}} \\
&\quad + \delta_{\text{C3(i)}}\delta_{H(i)} + 3\mu_i\delta_{H(i)} + 3\mu_i(2\mu_i + \epsilon_i), \\
A_3 &= \alpha_{1(i)}[-\beta_{H(i)}\left(\tau_{C(i)} + \delta_{\text{C3(i)}} + \tau_{H(i)} + 2\mu_i + \epsilon_i\right) + \tau_{C(i)}\delta_{H(i)} + \tau_{H(i)}[\tau_{C(i)} + \delta_{H(i)} + 2\mu_i + \epsilon_i] + 2\mu_i\tau_{C(i)} \\
&\quad + \epsilon_i\tau_{C(i)} + \delta_{\text{C3(i)}}\left(\delta_{H(i)} + \tau_{H(i)} + 2\mu_i + \epsilon_i\right) + 2\mu_i\delta_{H(i)} + 3\mu_i^2 + 2\mu_i\epsilon_i] - \beta_{H(i)}[(2\mu_i + \epsilon_i)\left(\tau_{C(i)} + \delta_{\text{C3(i)}}\right) \\
&\quad + \tau_{H(i)}\left(\tau_{C(i)} + \delta_{\text{C3(i)}} + 2\mu_i\right) + \mu_i(3\mu_i + 2\epsilon_i)] + \mu_i[\tau_{C(i)}[2\delta_{H(i)} + 3\mu_i + 2\epsilon_i] + \delta_{\text{C3(i)}}[2\delta_{H(i)} + 3\mu_i \\
&\quad + 2\epsilon_i] + \mu_i\left(3\delta_{H(i)} + 4\mu_i + 3\epsilon_i\right)] + \tau_{H(i)}[\tau_{C(i)}[\delta_{H(i)} + 2\mu_i + \epsilon_i] + \delta_{\text{C3(i)}}(\delta_{H(i)} + 2\mu_i + \epsilon_i) + \mu_i[2\delta_{H(i)} \\
&\quad + 3\mu_i + 2\epsilon_i], \\
A_4 &= \left(\alpha_{1(i)} + \mu_i\right)\left(\tau_{C(i)} + \delta_{\text{C3(i)}} + \mu_i\right)\left[\left(\tau_{H(i)} + \mu_i\right)\left[\delta_{H(i)} + \mu_i + \epsilon_i\right] - \beta_{H(i)}\left(\tau_{H(i)} + \mu_i + \epsilon_i\right)\right].
\end{aligned} \tag{24}$$

The Routh-Hurwitz criterion

A 4rd-degree polynomial $P(s) = a_4s^4 + a_3s^3 + a_2s^2 + a_1s + a_0$ is stable if and only if $a_4, a_3, a_4a_1 - a_3a_2, a_4a_0 - a_3a_1, a_2a_0 - a_1^2 > 0$.

Hence the E_0 is locally asymptotically stable if,

1. Clearly $A_4 = 1 > 0$ which is satisfied,
2. $A_1 > 0$,
3. $A_3 - A_1A_2 > 0$,
4. $A_4 - A_1A_3 > 0$ and,
5. $A_2A_4 - A_3^2 > 0$.

2.6. Sensitivity Analysis

The basic reproductive number R_0 also called propagation threshold of the model described by the system of differential equation 3 is very important in establishing efficient control measures. For its easiness to apply, Normalized Forward Sensitive Index method is used to determine the sensitivity indices as used in [21, 22]. It's index with regard to each parameter has been derived as follows to analyze the sensitivity of R_0 to any parameter(say μ_i),

$$\Omega_{\mu_i}^{R_0} = \frac{\partial R_0}{\partial \mu_i}\frac{\mu_i}{R_0}. \tag{25}$$

Where,

1. $\Omega_{\mu_i}^{R_0}$ is positive, increase in μ_i leads to increase in R_0 and,
2. $\Omega_{\mu_i}^{R_0}$ is negative, increase in μ_i leads to decrease in R_0.

The main goal of all control measures is to reduce the value of R_0 and to analyze the propagation threshold such that effective interventions can be determined. From the expression of the basic reproductive number in 2.5.3 and 25, the following is obtained:

$$\begin{aligned}
\Omega_{\beta_{H(i)}}^{R_0} &= \frac{\partial R_0}{\partial \beta_{H(i)}}\frac{\beta_{H(i)}}{R_0} = 1, \\
\Omega_{\tau_{T(i)}}^{R_0} &= \frac{\partial R_0}{\partial \tau_{T(i)}}\frac{\tau_{T(i)}}{R_0} = -\frac{\tau_{T(i)}}{\mu_i + \delta_{T(i)} + \tau_{T(i)}}, \\
\Omega_{\alpha_{1(i)}}^{R_0} &= \frac{\partial R_0}{\partial \alpha_{1(i)}}\frac{\alpha_{1(i)}}{R_0} = \frac{\mu_i}{\alpha_{1(i)} + \mu_i}, \\
\Omega_{\beta_{T(i)}}^{R_0} &= \frac{\partial R_0}{\partial \beta_{T(i)}}\frac{\beta_{T(i)}}{R_0} = 1, \\
\Omega_{\delta_{T(i)}}^{R_0} &= \frac{\partial R_0}{\partial \delta_{T(i)}}\frac{\delta_{T(i)}}{R_0} = -\frac{\delta_{T(i)}}{\mu_i + \delta_{T(i)} + \tau_{T(i)}},
\end{aligned}$$

$$
\begin{aligned}
\Omega^{R_0}_{\delta_{H(i)}} &= \frac{\partial R_0}{\partial \delta_{H(i)}}\frac{\delta_{H(i)}}{R_0} = -\frac{\delta_{H(i)}}{\delta_{H(i)}+\mu_i+\epsilon_i},\\
\Omega^{R_0}_{\eta_i} &= \frac{\partial R_0}{\partial \eta_i}\frac{\eta_i}{R_0} = \frac{\eta_i\epsilon_i\tau_{H(i)}}{h_9},\\
\Omega^{R_0}_{\epsilon_i} &= \frac{\partial R_0}{\partial \epsilon_i}\frac{\epsilon_i}{R_0} = \frac{\epsilon_i\left(\delta_{H(i)}h_{10}+(\eta_i-1)\mu_i\tau_{H(i)}\right)}{\left(\delta_{H(i)}+\mu_i+\epsilon_i\right)(h_9)},\\
\Omega^{R_0}_{\tau_{H(i)}} &= \frac{\partial R_0}{\partial \tau_{H(i)}}\frac{\tau_{H(i)}}{R_0} = \frac{(\eta_i-1)\epsilon_i(d_i+\mu_i)\tau_{H(i)}}{\left(d_i+\tau_{H(i)}+\mu_i\right)(h_9)},\\
\Omega^{R_0}_{d_i} &= \frac{\partial R_0}{\partial d_i}\frac{d_i}{R_0} = -\frac{d_i(\eta_i-1)\epsilon_i\tau_{H(i)}}{\left(d_i+\tau_{H(i)}+\mu_i\right)(h_9)},\\
\Omega^{R_0}_{\mu_i} &= \frac{\partial R_0}{\partial \mu_i}\frac{\mu_i}{R_0} = -\mu_i\left(\frac{1}{d_i+\tau_{H(i)}+\mu_i}+\frac{1}{\delta_{H(i)}+\mu_i+\epsilon_i}\right)+\frac{-d_i\epsilon_i-\eta_i\epsilon_i\tau_{H(i)}+\mu_i^2}{h_9},
\end{aligned}
\tag{26}
$$

where $h_9 = (d_i+\mu_i)(\mu_i+\epsilon_i)+\tau_{H(i)}(\mu_i+\eta_i\epsilon_i)$ and $h_{10} = \left(d_i+\eta_i\tau_{H(i)}+\mu_i\right)$.

3. Results and Discussions

In this section, approximate solutions to the model equations 3 are found using $\mathcal{O}(h^4)$ and $\mathcal{O}(h^5)$ order Runge-Kutta methods which are implemented via the solve_ivp() function from Scipy library in Python. The initial populations are given by,

$$
\begin{aligned}
&\{N_0 = 10000, S_0 = 9850, D_0 = 10, I_0 = 5, U_0 = A_0 = 0,\\
&E_0 = R_0 = C_{LU0} = C_{LH0} = C_{TH0} = 0\} \text{ and}\\
&\{N_0 = 10000, S_0 = 9850, D_0 = 100, I_0 = 50,\\
&U_0 = A_0 = E_0 = R_0 = C_{LU0} = C_{LH0} = C_{TH0} = 0\},
\end{aligned}
\tag{27}
$$

for children (0-14 years) and adults (above 15 years) respectively.

3.1. *Fitting Graphs and Parameters Estimation*

This study used HIV data from UNAIDS that was available online at HIV estimates with uncertainty bounds from 1991 to present. It gives Global HIV & AIDS statistics for different countries including Kenya. TB data was available from NLTP accessible at DSTB Dashboard. TB data was available from 2015 to 2023. The data was prepared using Python by filtering Kenya data only and also reorganizing the columns by renaming.

Given the data points,

$$(t_1, y_1), (t_2, y_2), ..., (t_n, y_n), \tag{28}$$

least squares method is used to find the parameter value $\hat{P}$ such that the approximate solution $\hat{y} = f(t, \hat{P})$ gives the squared sum of errors(SSE):

$$SSE(\hat{P}) = \sum_{i=1}^{n}(y_i - f(t_i, \hat{P}))^2. \tag{29}$$

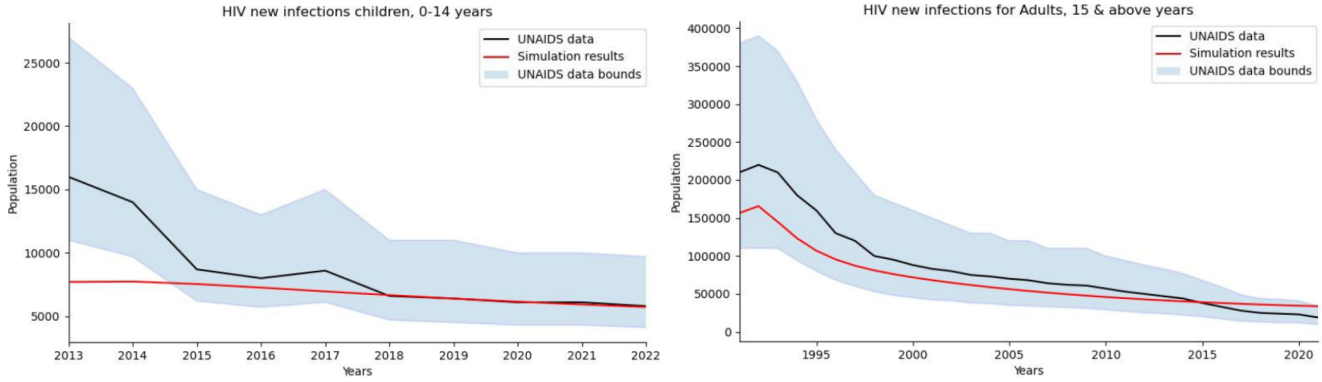

(a) Children: $\beta_{H(1)} = 0.17, \epsilon_1 = 0.676$ *and* $SSE = 17430.58$ *(b) Adults:* $\beta_{H(2)} = 0.29, \epsilon_2 = 0.78$ *and* $SSE = 612814.91$

Figure 2. *Fitting graphs for HIV new infections in the HIV diagnosed classes,* D_i *&* $C_{LU(i)}$*, compared with UNAIDS data.*

The best approximate solution $\hat{y}^*$ is picked after minimizing SSE such that,

$$SSE(\hat{P}^*) = \min_{i=0}^{n}\{SSE_i(\hat{P})\} \text{ and } \hat{y}^* = f(t, \hat{P}^*). \tag{30}$$

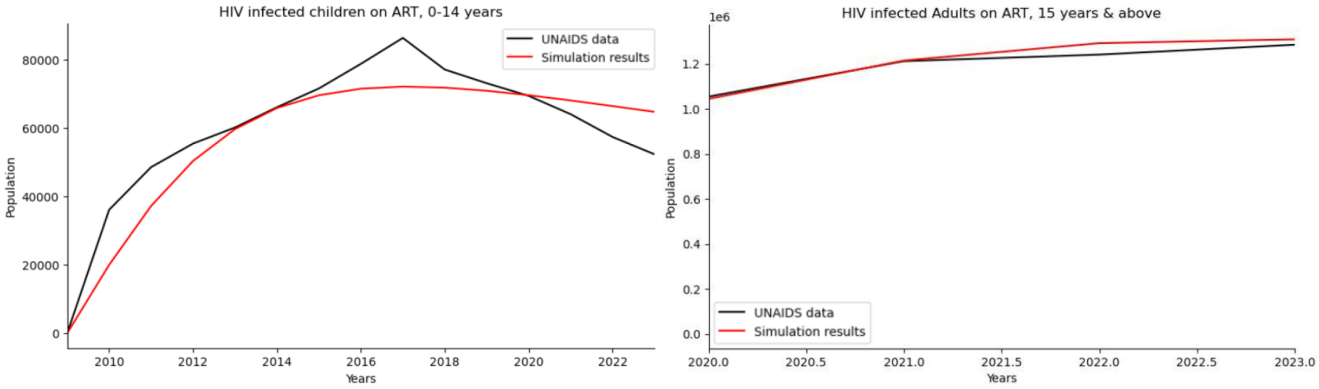

(a) Children: $\tau_{H(1)} = 0.8, \tau_{C(1)} = 0.67, d_1 = 0.4$ *and* $SSE = 77398.29$ *(b) Adults:* $\tau_{H(2)} = 0.75, \tau_{C(2)} = 0.65, d_2 = 0.25$ *and* $SSE = 63704.94$

Figure 3. *Fitting graphs for people living with HIV who are on ART, A_i, compared with UNAIDS data.*

Using least squares method, figures 2, 3 and 4 are some of the fitting graphs that were obtained with their respective parameters and SSE as described at (29).

The parameter values are presented on table 2 and 3 for children and adults respectively. They are based on Least Square Method(LSM), previous study sources and estimation.

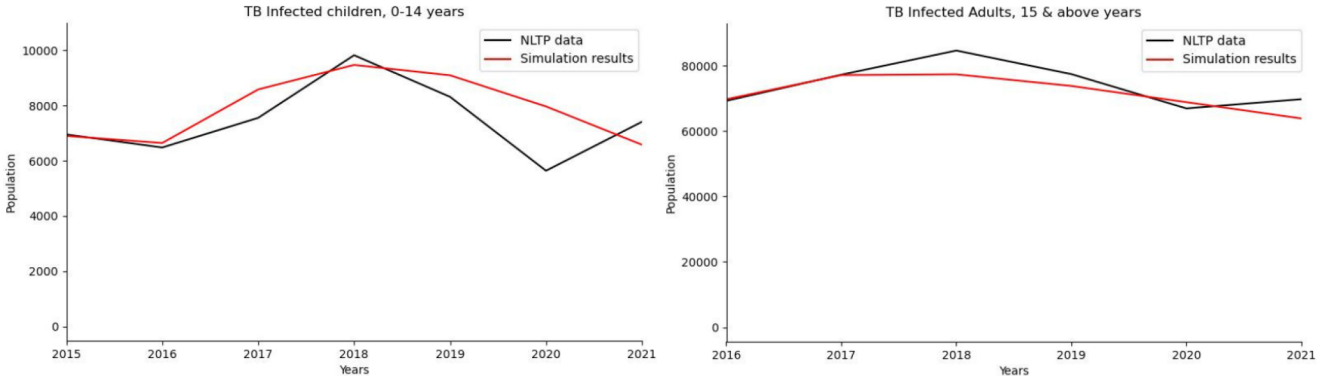

(a) Children: $\beta_{T(1)} = 0.31, \alpha_{1(1)} = 0.3, \alpha_{2(1)} = 0.6$ *and* $SSE = 10763.41$ *(b) Adults:* $\beta_{T(2)} = 0.33, \alpha_{1(2)} = 0.25, \alpha_{2(2)} = 0.5$ *and* $SSE = 13421.10$

Figure 4. *Fitting graphs for those infected with TB, compared with NLTP data.*

Throughout the fitting process, there are parts of the curve that fit well while there are parts that do not fit well. The latter is caused by non-uniform data distribution or different behaviors in the data. This study would recommend assessing polynomial fitting, spline fitting, or other nonlinear models. Data points that are far from the curve (outliers) and have unusual large residuals disproportionately affect the least squares fit. The outliers should be determined if they are measurement errors or genuinely part of the data. Also, robust fitting techniques are recommended, like least absolute deviation or weighted least squares.

3.2. Sensitivity Analysis

In epidemic modeling, sensitivity analysis is performed to investigate model parameters with significant influence on R_0 and hence on the transmission and the spread of the disease under study [23]. The model sensitivity analysis in this study is used to investigate parameter influence on the dynamics of HIV, TB and both HIV & TB infected population under different conditions on the reproduction number, R_0. In order to eliminate the HIV-TB co-infection infection, the reproduction number should be less than one, that is, $R_0 < 1$.

From table 4, a positive sign on the SI indicates that an increase in the value of such a parameter increases the value of R_0 and hence the growth of infected infection. On the other hand, a negative sign is indicative of a parameter that negatively affects R_0.

Table 2. *Estimated parameters for children aged 0-14 years:* $y^{-1} = year^{-1}$.

Par	Value	Source	Interval	Units
π_1	0.028N	[2,6]	$(0.028N, 0.0409N)$	y^-1
$\beta_{H(1)}$	0.17	LSM	$(0.17, 0.2)$	y^-1
$\beta_{T(1)}$	0.31	LSM	$(0.25, 0.31)$	y^-1
μ_1	0.04	*	$(0.045, 0.055)$	y^-1
ϵ_1	0.676	LSM	$(0.6, 0.8)$	y^-1
$\alpha_{1(1)}$	0.3	LSM	$(0.25, 0.4)$	y^-1
$\alpha_{2(1)}$	0.6	LSM	$(0.5, 0.65)$	y^-1
$\tau_{H(1)}$	0.79	LSM	$(0.75, 0.95)$	y^-1
$\tau_{T(1)}$	0.58	NLTP	$(0.55, 0.6)$	y^-1
$\tau_{C(1)}$	0.78	LSM	$(0.67, 0.8)$	y^-1
θ_1	0.0001	[1]	$(0.0001, 0.9)$	y^-1
η_1	1-0.65	[4]	1-$(0.5, 0.82)$	y^-1
d_1	0.4	LSM	$(0.2, 0.5)$	y^-1
$\delta_{H(1)}$	0.06	*	$(0.05, 0.08)$	y^-1
$\delta_{T(1)}$	0.1	*	$(0.08, 0.12)$	y^-1
$\delta_{C1(1)}$	0.14	*	$(0.1, 0.16)$	y^-1
$\delta_{C1(1)}$	0.14	*	$(0.1, 0.16)$	y^-1
$\delta_{C1(1)}$	0.24	*	$(0.2, 0.26)$	y^-1

1 - [24], 2- [25], 4 - UNAIDS, 6 - [26], & * - Assumed.

Table 3. *Parameters value used in numerical simulations for adults:* $year^{-1} = y^{-1}$.

Par	Value	Source	Interval	Units
π_2	0.0355N	[3,6]	$(0.028N, 0.0409N)$	y^-1
$\beta_{H(2)}$	0.29	LSM	$(0.21, 0.29)$	y^-1
$\beta_{T(2)}$	0.33	LSM	$(0.25, 0.33)$	y^-1
μ_2	0.06	*	$(0.06, 0.07)$	y^-1
ϵ_2	0.78	LSM	$(0.62, 0.9)$	y^-1
$\alpha_{1(2)}$	0.25	LSM	$(0.2, 0.29)$	y^-1
$\alpha_{2(2)}$	0.5	LSM	$(0.4, 0.58)$	y^-1
$\tau_{H(2)}$	0.75	LSM	$(0.65, 0.8))$	y^-1
$\tau_{T(2)}$	0.4	*	$(0.4, 0.6)$	y^-1
$\tau_{C(2)}$	0.65	LSM	$(0.6, 0.69)$	y^-1
θ_2	0.0001	[1]	$(0.0001, 0.9)$	y^-1
η_2	1-0.75	[4]	1-$(0.75, 0.98)$	y^-1
d_2	0.25	LSM	$(0.23, 0.3)$	y^-1
$\delta_{H(2)}$	0.08	*	$(0.07, 0.1)$	y^-1
$\delta_{T(2)}$	0.1	[1]	$(0.09, 0.12)$	y^-1
$\delta_{C1(2)}$	0.16	*	$(0.14, 0.18)$	y^-1
$\delta_{C1(2)}$	0.16	*	$(0.14, 0.18)$	y^-1
$\delta_{C1(2)}$	0.26	[8]	$(0.24, 0.28)$	y^-1

1 - [24], 3- [25], 4 - UNAIDS, 6 - [26], 8 - [27] & * - Assumed.

Table 4. *Sensitivity Indices: 1 - Children and 2 - Adults.*

Par	SI(0-14)	SI(>15)	Desc
$\beta_{H(i)}$	+1	+1	$\beta_{H(1)}, \beta_{H(2)} \sim R_0$
$\beta_{T(i)}$	+1	+1	$\beta_{T(1)}, \beta_{T(2)} \sim R_0$
$\alpha_{1(i)}$	+0.117647	+0.193548	$\alpha_{1(1)}\alpha_{1(2)} \sim R_0$
$\delta_{H(i)}$	-0.0773196	-0.0869565	$\delta_{H(1)}, \delta_{H(2)} \sim \frac{1}{R_0}$
$\delta_{T(i)}$	-0.138889	-0.178571	$\delta_{T(1)}, \delta_{T(2)} \sim \frac{1}{R_0}$
$\tau_{H(i)}$	-0.232732	-0.2841	$\tau_{H(1)}, \tau_{H(2)} \sim \frac{1}{R_0}$
$\tau_{T(i)}$	-0.805556	-0.714286	$\tau_{T(1)}, \tau_{T(2)} \sim \frac{1}{R_0}$
η_i	+0.350319	+0.323813	$\eta_1, \eta_2 \sim R_0$
d_i	+0.211575	+0.229113	$d_1, d_2 \sim R_0$
ϵ_i	+0.03665	+0.01136	$\epsilon_1, \epsilon_2 \sim R_0$
μ_i	-0.938177	-0.869413	$\mu_1, \mu_2 \sim \frac{1}{R_0}$

3.3. Optimal Control Model

In order to control the co-infection, the system (3) is extended into an optimal control problem by incorporating two time-dependent control functions. These control functions are introduced at a specified time t with $t \in [0, T]$, as follows, where T is the final time.

1. $u_1(t)$: *TB treatment*. TB should be treated early in order to prevent its progression. The CDC recommends 12 weeks of once-weekly isoniazid and rifapentine for people with latent TB infection and HIV who are taking antiretroviral medications that don't interact with rifapentine [28].
2. $u_2(t)$: *ART adherence.* For ART to suppress viral replication and remain effective over time, high levels of patient adherence are needed [29].

Including the control measures u_1 and u_2 in the model 3, the following optimal control model is got,

$$\begin{aligned}
\frac{dS_i}{dt} &= \pi_{(i)} - \left(\lambda_{H(i)} + \lambda_{T(i)} + \mu_i\right) S_i,\\
\frac{dU_i}{dt} &= \lambda_{H(i)} S_i - (\lambda_{T(i)} + \epsilon_i + \delta_{H(i)} + \mu_{(i)}) U_i,\\
\frac{dD_i}{dt} &= \epsilon_{(i)} U_{i(i)} + (1-u_2) d_{(i)} A_i - \left(\lambda_{T(i)} + \tau_{H(i)} + \mu_{(i)}\right) D_i,\\
\frac{dA_i}{dt} &= D_i \tau_{H(i)} + (C_{LHi} + C_{THi}) u_1 \tau_{C(i)} - \left(\mu_{(i)} + (1-u_2) d_{(i)}\right) A_i,\\
\frac{dE_i}{dt} &= \lambda_{T(i)} S_i + \theta_{(i)} R_i - \left(\alpha_{1(i)} + \lambda_{H(i)} + \mu_{(i)}\right) E_i,\\
\frac{dI_i}{dt} &= \alpha_{1(i)} E_i - \left(\lambda_{H(i)} + u_1 \tau_{T(i)} + \delta_{T(i)} + \mu_{(i)}\right) I_i,\\
\frac{dR_i}{dt} &= u_1 \tau_{T(i)} I_i - \left(\theta_{(i)} + \mu_{(i)}\right) R_i,
\end{aligned} \tag{31}$$

$$\begin{aligned}
\frac{dC_{LU(i)}}{dt} &= \lambda_{T(i)} U_i + \lambda_{H(i)} E_i - \left(\epsilon_{(i)} + \delta_{C1(i)} + \mu_{(i)}\right) C_{LU(i)},\\
\frac{dC_{LH(i)}}{dt} &= \epsilon_{(i)} C_{LU(i)} + \lambda_{T(i)} D_i - [u_1 \tau_{C(i)} + (1-u_1)\alpha_{2(i)} + \delta_{C2(i)} + \mu_{(i)}] C_{LH(i)},\\
\frac{dC_{TH(i)}}{dt} &= (1-u_1)\alpha_{2(i)} C_{LHi} + \lambda_{H(i)} I_i - [u_1 \tau_{C(i)} + \delta_{C3(i)} + \mu_{(i)}] C_{TH(i)}.
\end{aligned} \tag{32}$$

The initial conditions satisfy,

$$\begin{aligned}
&S_{i0} \geq 0,\ U_{i0} \geq 0,\ D_{i0} \geq 0,\ A_{i0} \geq 0,\ E_{i0} \geq 0,\ I_{i0} \geq 0,\\
&R_{i0} \geq 0,\ C_{LUi0} \geq 0,\ C_{LHi0} \geq 0,\ C_{THi0} \geq 0.
\end{aligned} \tag{33}$$

The Lebesgue measurable control set U is defined as follows in order to investigate the optimal control levels,

$$U = \{(u_1(t), u_2(t)) : 0 \leq u_1 \leq 1, 0 \leq u_2 \leq 1, 0 \leq t \leq t_f)\}, \tag{34}$$

where t_f is the end time of implementing controls. The population of HIV diagnosed, Active TB and co-infection TB & HIV is minimized by finding the optimal controls u_1^* and u_2^* that leads to the following objective function,

$$J(u_1,u_2)=\min_{(u_1,u_2)}\int_0^{t_f} c_1D_{(i)}+c_2I_{(i)}+c_3C_{LH(i)}+c_4C_{TH(i)}+\frac{1}{2}(w_1u_1^2+w_2u_2^2)dt, \tag{35}$$

where $c_1, c_2, c_3, c_4, w_1,$ and w_2 are constants. Equations $\frac{1}{2}w_1u_1^2$ and $\frac{1}{2}w_2u_2^2$ are the costs associated with the controls. The goal is to find the optimal controls u_1^* and u_2^* and optimal solutions by fixing the terminal time t_f that minimize the objective functional such that,

$$J(u_1^*,u_2^*)=\min\{J(u_1,u_2):u_1,u_2\in U\}. \tag{36}$$

3.4. Existence of the Optimal Control

To show the existence of optimal control, the approach by [30] is used. It is already proved that the system (3) is bounded, so this result can be used to prove the existence of optimal control over finite time interval as applied in [30, 31]. To ensure the existence of optimal control, following conditions must be checked if they are satisfied:

1. The set of controls and state variables be nonempty.
2. The control set U is convex and closed.
3. The right hand side of the state system is bounded by a linear function in the state and control variables.
4. The integrand of objective functional is convex on U.
5. The integrand of objective functional is bounded below by $k_2-k_1\left(|u_1|^2+|u_2|^2\right)^{k/2}, k_1,k_2>0$ and $k>1$.

An existence of the state system with bounded coefficients has been used to give condition (i). The control set is convex and closed by definition hence (ii). The right hand side of the state system satisfies (iii). The state solutions are already bounded (iv). The integrand in the objective functional $c_1D_{(i)}+c_2I_{(i)}+c_3C_{LH(i)}+c_4C_{TH(i)}+\frac{1}{2}(w_1u_1^2+w_2u_2^2)$ is clearly convex in U. For (v), from the bounds of the control system,

$$\frac{1}{2}w_iu_i^2\le\frac{1}{2}w_i, u_i\in[0,1]. \tag{37}$$

Also, considering the preceding inequality, the integrand can be written as

$$c_1D_{(i)}+c_2I_{(i)}+c_3C_{LH(i)}+c_4C_{TH(i)}+\frac{1}{2}(w_1u_1^2+w_2u_2^2)\ge k_1\left(|u_1|^2+|u_2|^2\right)^{k/2}-k_2, \tag{38}$$

where $k_1=\min(w_1/2,w_2/2), k_2=w_2/2, k=2$. Therefore, there exists optimal control measures u_1 and u_2 that minimize the objective functional $J(u_1,u_2)$.

3.5. The Hamiltonian and Optimality System

The Pontryagin maximum principle stated the necessary conditions which are satisfied by optimal pair. Hence, by this principle, the Hamiltonian function (H) is obtained and defined as,

$$\begin{aligned}
H\left(S_{(i)},...,C_{TH(i)}\right)&=c_1D_{(i)}+c_2I_{(i)}+c_3C_{LH(i)}+c_4C_{TH(i)}\\
&+\frac{1}{2}(w_1u_1^2+w_2u_2^2)+\lambda_1\{\pi_{(i)}-\left(\lambda_{H(i)}+\lambda_{T(i)}+\mu_i\right)S_i\}\\
&+\lambda_3\{\epsilon_{(i)}U_{i(i)}+(1-u_2)d_{(i)}A_i-\left(\lambda_{T(i)}+\tau_{H(i)}+\mu_{(i)}\right)D_i\}\\
&+\lambda_4\{D_i\tau_{H(i)}+(C_{LHi}+C_{THi})u_1\tau_{C(i)}-[\mu_{(i)}+(1-u_2)\\
&d_{(i)}]A_i\}+\lambda_5\{\lambda_{T(i)}S_i+\theta_{(i)}R_i-\left(\alpha_{1(i)}+\lambda_{H(i)}+\mu_{(i)}\right)E_i\}\\
&+\lambda_6\{\alpha_{1(i)}E_i-\left(\lambda_{H(i)}+u_1\tau_{T(i)}+\delta_{T(i)}+\mu_{(i)}\right)I_i\}\\
&+\lambda_7\{u_1\tau_{T(i)}I_i-\left(\theta_{(i)}+\mu_{(i)}\right)R_i\}+\lambda_8\{\lambda_{T(i)}U_i+\lambda_{H(i)}E_i\\
&-\left(\epsilon_{(i)}+\delta_{C1(i)}+\mu_{(i)}\right)C_{LU(i)}\}+\lambda_9\{\epsilon_{(i)}C_{LU(i)}+\lambda_{T(i)}D_i\\
&-\left(u_1\tau_{C(i)}+(1-u_1)\alpha_{2(i)}+\delta_{C2(i)}+\mu_{(i)}\right)C_{LH(i)}\}\\
&+\lambda_{10}\{(1-u_1)\alpha_{2(i)}C_{LHi}+\lambda_{H(i)}I_i-\\
&\left(u_1\tau_{C(i)}+\delta_{C3(i)}+\mu_{(i)}\right)C_{TH(i)}\}.
\end{aligned} \tag{39}$$

Where, $\lambda_i, i=1,...,10$ are the adjoint variables corresponding to state variables $S_{(i)}, U_{(i)}, ...$ and $C_{TH(i)}$, respectively, and to be determined using Pontryagins maximal principle for the existence of optimal pairs.

Theorem 3.1. Let $S_{(i)}, U_{(i)}, D_{(i)}, A_{(i)}, E_{(i)}, I_{(i)}, R_{(i)}, C_{LU(i)}, C_{LH(i)}$ and $C_{TH(i)}$ be optimal state solutions with associated

optimal control variables u_1 and u_2 for the optimal control model, there exist co-state variables $\lambda_1, ..., \lambda_9$ that satisfy,

$$\begin{aligned} \frac{d_i\lambda_1}{dt} &= -\frac{\partial H}{\partial S_{(i)}}, \frac{d_i\lambda_2}{dt} = -\frac{\partial H}{\partial U_{(i)}}, \frac{d_i\lambda_3}{dt} = -\frac{\partial H}{\partial D_{(i)}}, \\ \frac{d_i\lambda_4}{dt} &= -\frac{\partial H}{\partial A_{(i)}}, \frac{d_i\lambda_5}{dt} = -\frac{\partial H}{\partial E_{(i)}}, \frac{d_i\lambda_6}{dt} = -\frac{\partial H}{\partial I_{(i)}}, \end{aligned} \tag{40}$$

$$\frac{d_i\lambda_7}{dt} = -\frac{\partial H}{\partial R_{(i)}}, \frac{d_i\lambda_8}{dt} = -\frac{\partial H}{\partial C_{LU(i)}}, \frac{d_i\lambda_9}{dt} = -\frac{\partial H}{\partial C_{LH(i)}}, \frac{d_i\lambda_{10}}{dt} = -\frac{\partial H}{\partial C_{TH(i)}}.$$

With transversality or final time conditions, $\lambda_1(t_f) = ... = \lambda_{10}(t_f) = 0$, and where H is Hamiltonian function given in $(*)$. Furthermore, the optimal controls u_1^*, and u_2^* are,

$$\begin{aligned} u_1^* &= \min\left\{1, \max\left\{\phi_1\right\}, 0\right\}, \\ u_2^* &= \min\left\{1, \max\left\{\frac{(\lambda_3 + \lambda_4)d_{(i)}A_{(i)}}{w_2}\right\}, 0\right\}. \end{aligned} \tag{41}$$

Where,

$$\phi_1 = \frac{(\lambda_4 - \lambda_{10})\tau_{C(i)}C_{TH(i)} + \{(\lambda_4 - \lambda_9)\tau_{C(i)} + \frac{(\lambda_9 - \lambda_{10})\alpha_{2(i)}\}C_{LH(i)} + (\lambda_7 - \lambda_6)\tau_T I_{(i)}}{w_1}.$$

Proof. Pontryagins maximum principle gives the standard form of adjoint equation with transversality conditions [31]. The standard results in [32] are applied to derive the adjoint relations, the transversality conditions and the optimal control system. Now, differentiating the Hamiltonian function with respect to state variables $S_{(i)}, U_{(i)}, ...$ and $C_{TH(i)}$, respectively, the adjoint equations can be written as,

$$\begin{aligned} \frac{d_i\lambda_1}{dt} &= -\frac{\partial H}{\partial S_i} = \lambda_1(\lambda_{H(i)} + \lambda_{T(i)} + \mu_i) - \lambda_2\lambda_{H(i)} - \lambda_5\lambda_{T(i)}, \\ \frac{d_i\lambda_2}{dt} &= -\frac{\partial H}{\partial U_i} = \lambda_2(\lambda_{T(i)} + \epsilon_i + \delta_{H(i)} + \mu_{(i)}) - \lambda_3\epsilon_{(i)} - \lambda_8\lambda_{T(i)}, \\ \frac{d_i\lambda_3}{dt} &= -\frac{\partial H}{\partial D_i} = -c_1 - \left(\lambda_{T(i)} + \tau_{H(i)} + \mu_{(i)}\right) - \lambda_4\tau_{H(i)} - \lambda_9\lambda_{T(i)}, \\ \frac{d_i\lambda_4}{dt} &= -\frac{\partial H}{\partial A_i} = -\lambda_3(1 - u_2)d_{(i)} + \lambda_4\left(\mu_{(i)} + (1 - u_2)d_{(i)}\right), \\ \frac{d_i\lambda_5}{dt} &= -\frac{\partial H}{\partial E_i} = \lambda_5\left(\alpha_{1(i)} + \lambda_{H(i)} + \mu_{(i)}\right) + \lambda_6\alpha_{1(i)} + \lambda_8\lambda_{H(i)}, \\ \frac{d_i\lambda_6}{dt} &= -\frac{\partial H}{\partial I_i} = -c_2 + \lambda_6\left(\lambda_{H(i)} + u_1\tau_{T(i)} + \delta_{T(i)} + \mu_{(i)}\right) - \lambda_7 u_1\tau_{T(i)} + \lambda_{10}\lambda_{H(i)}, \end{aligned}$$

$$\begin{aligned} \frac{d_i\lambda_7}{dt} &= -\frac{\partial H}{\partial R_i} = -\lambda_5\theta_{(i)} + \lambda_7(\theta_{(i)} + \mu_{(i)}), \\ \frac{d_i\lambda_8}{dt} &= -\frac{\partial H}{\partial C_{LU(i)}} = \lambda_8\left(\epsilon_{(i)} + \delta_{C1(i)} + \mu_{(i)}\right) + \lambda_9\epsilon_{(i)}, \\ \frac{d_i\lambda_9}{dt} &= -\frac{\partial H}{\partial C_{LH(i)}} = -c_3 - \lambda_4 u_1\tau_{C(i)} + \lambda_9[u_1\tau_{C(i)} + (1 - u_1)\alpha_{2(i)} + \delta_{C2(i)} + \mu_{(i)}] - \lambda_{10}(1 - u_1)\alpha_{2(i)}, \end{aligned}$$

$$\frac{d_i\lambda_{10}}{dt} = -\frac{\partial H}{\partial C_{TH(i)}} = -c_4 - \lambda_4 u_1\tau_{C(i)} + \lambda_{10}\left(u_1\tau_{C(i)} + \delta_{C3(i)} + \mu_{(i)}\right).$$

Further, the characterization of optimal controls u_1^*, and u_2^* shows that,

$$\frac{\partial H}{\partial u_1} = \frac{\partial H}{\partial u_2} = 0. \tag{42}$$

It follows that the optimal solution subject to constraints $0 \leq u_1 \leq 1, 0 \leq u_2 \leq 1$ is,

$$\begin{aligned} u_1^* = u_1 &= \frac{(\lambda_4 - \lambda_{10})\tau_{C(i)} C_{TH(i)} + \{(\lambda_4 - \lambda_9)\tau_{C(i)}}{w_1} + \frac{(\lambda_9 - \lambda_{10})\alpha_{2(i)}\} C_{LH(i)} + (\lambda_7 - \lambda_6)\tau_T I_{(i)}}{w_1}, \\ u_2^* = u_2 &= \frac{(\lambda_3 + \lambda_4) d_{(i)} A_{(i)}}{w_2}. \end{aligned} \tag{43}$$

Using the equation (42), and the lower and upper bounds of four control measures, we obtained the characterization of optimal controls as follows.

$$u_1^* \in U \implies u_1^* = \begin{cases} 0, \text{ if } \phi_1 < 0, \\ \phi_1, \text{ if } 0 \leq \phi_1 \leq 1, \text{ and} \\ 1, \text{ if } \phi_1 > 1. \end{cases} \tag{44}$$

$$u_2^* \in U \implies u_2^* = \begin{cases} 0, \text{ if } \phi_2 < 0, \\ \phi_2, \text{ if } 0 \leq \phi_2 \leq 1, \\ 1, \text{ if } \phi_2 > 1. \end{cases} \tag{45}$$

Where,

$$\phi_2 = \frac{(\lambda_3 + \lambda_4) d_{(i)} A_{(i)}}{w_2}.$$

In compact form, the optimal controls can be written as,

$$\begin{aligned} u_1^* = u_1 &= \min\{1, \max\{\phi_1\}, 0\}, \\ u_2^* = u_2 &= \min\{1, \max\{\phi_2\}, 0\}. \end{aligned} \tag{46}$$

3.6. Graphs for Children, 0-14 Years

In order to illustrate the feasibility of the theoretical results and the control strategies, graphs emanating from the numerical simulations are given. The python library, Matplotlib, is used to make the plots showing children$(0 - 14)$ population dynamics over time.

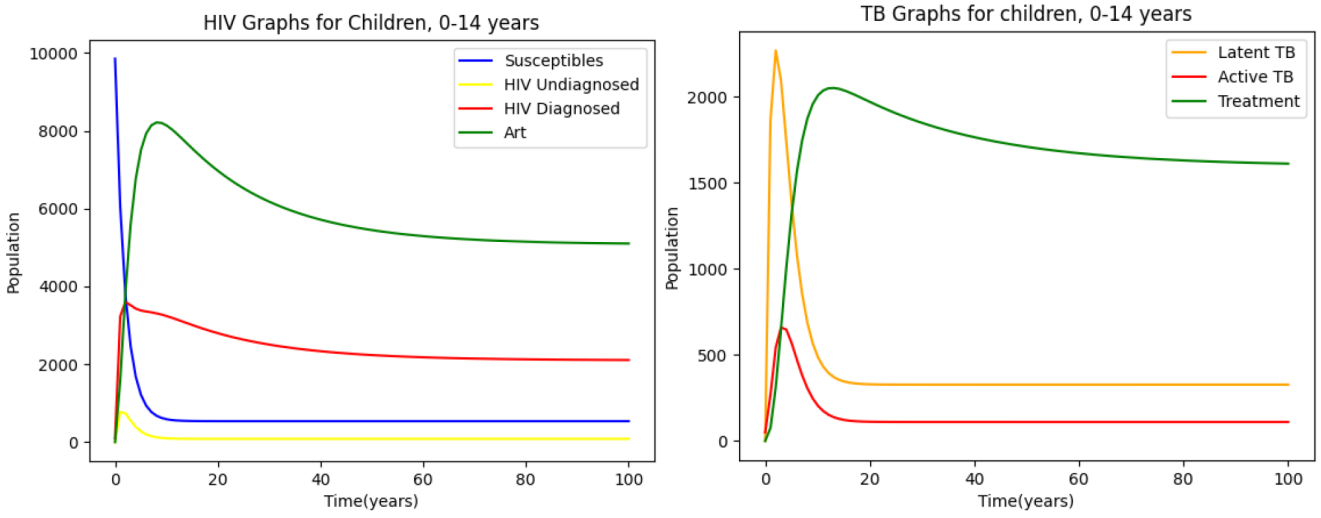

(a) HIV sub-model graphs for children, 0 - 14 years.

(b) TB sub-model graphs for children, 0 - 14 years.

Figure 5. *Children dynamics for the sub-models.*

In figure 5, the HIV and TB submodel dynamics for children are presented. It can be seen that in figure 5a that the susceptible population decreases drastically due to $R_0 = 2.376 > 1$. HIV undiagnosed, diagnosed and ART populations increase drastically in the initial 20 years. It can be noted that the population for the undiagnosed is lower compared to $D_i \& A_i$ populations due to the high rate of testing. All populations stabilize past 50 years.

Figure 5b presents the dynamics for TB among children. Latent and Active TB populations increases fast in the first 10 years but later it goes down to stabilize at about 17 years. TB treatment population increases over the first 17 years then

it goes down slowly since the Active TB class has stabilized. There is minimum population change beyond 60 years.

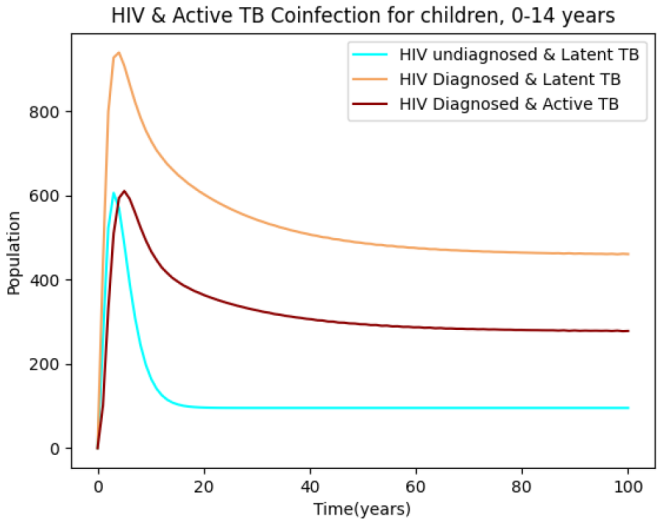

Figure 6. *Co-infection graphs for children, 0 - 14 years.*

The co-infection graphs for children are presented by the figure 6. All the three graphs increase to reach their maxima during the beginning 5 years then the populations decrease slowly to later stabilize past 60 years. Notably, the populations for co-infection of latent TB with undiagnosed and diagnosed HIV attain almost the same maxima due to the high rate of HIV testing, $\epsilon = 0.676$

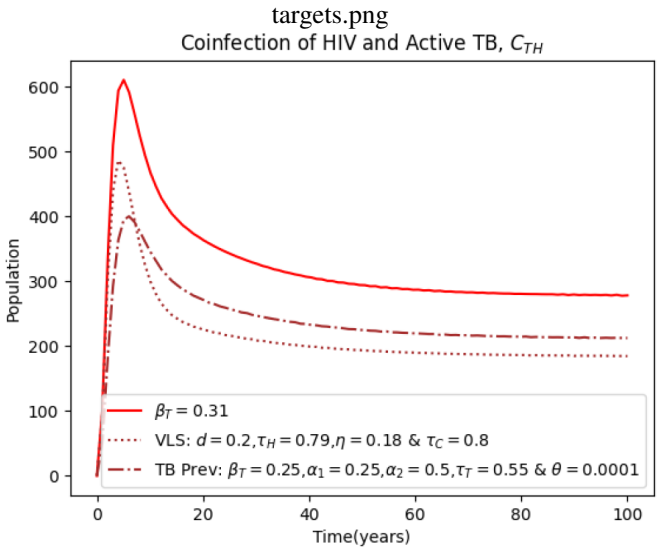

Figure 7. *Interventions comparison between viral load suppression and TB prevention on children population.*

On figure 7, an intervention comparison between viral load suppression and TB prevention are presented. While it is vividly clear that both the interventions reduce the co-infection population (Active TB and HIV), the simulations show that viral load suppression is more effective for children. As many as 40% of the 1 million children living with HIV (CLHIV) and receiving antiretroviral treatment (ART), have not achieved viral suppression [33].

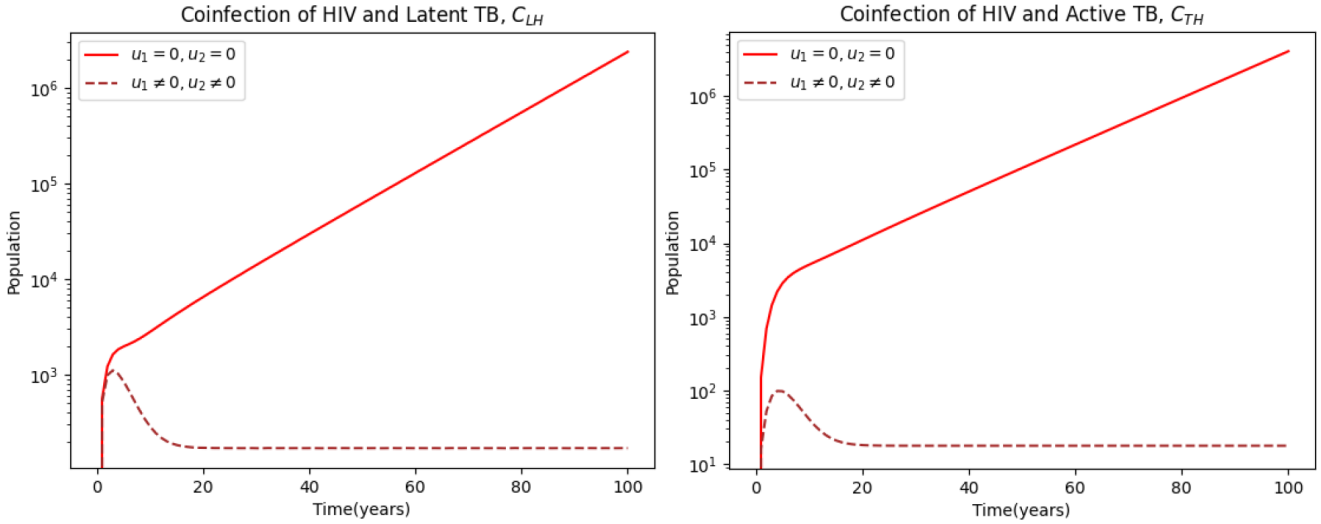

Figure 8. *Comparison of co-infection population without and with control for children (log-scale y-axis).*

Figure 8 presents the coinfection population dynamics for children considering the TB treatment and HIV adherence control interventions. The coinfections population sizes remain small due to intervention with controls. However, without controls, more people severely attacked with HIV & TB hence they progress to advanced stages so that the sizes of the coinfection populations population increases over time.

Figure 9 compares the effect of the two control strategies in the coinfected populations. The graph on left shows that ART adherence is the most effective intervention for children infected with latent TB and HIV. TB treatment is the most effective intervention for children infected with active TB and HIV as shown in the graph or the right.

Figure 10 displays the comparison of the original

coinfection dynamics presented at 6 with the dynamics with optimal control. The optimal controls do not have instant significance for coinfection of HIV and latent TB, $C_{LH(i)}$ population but have great longterm significance in reducing $C_{LH(i)}$ population size as displayed on the graph of 10-left. The optimal controls have instant and significance reduction for coinfection of HIV and active TB, $C_{TH(i)}$ population size.

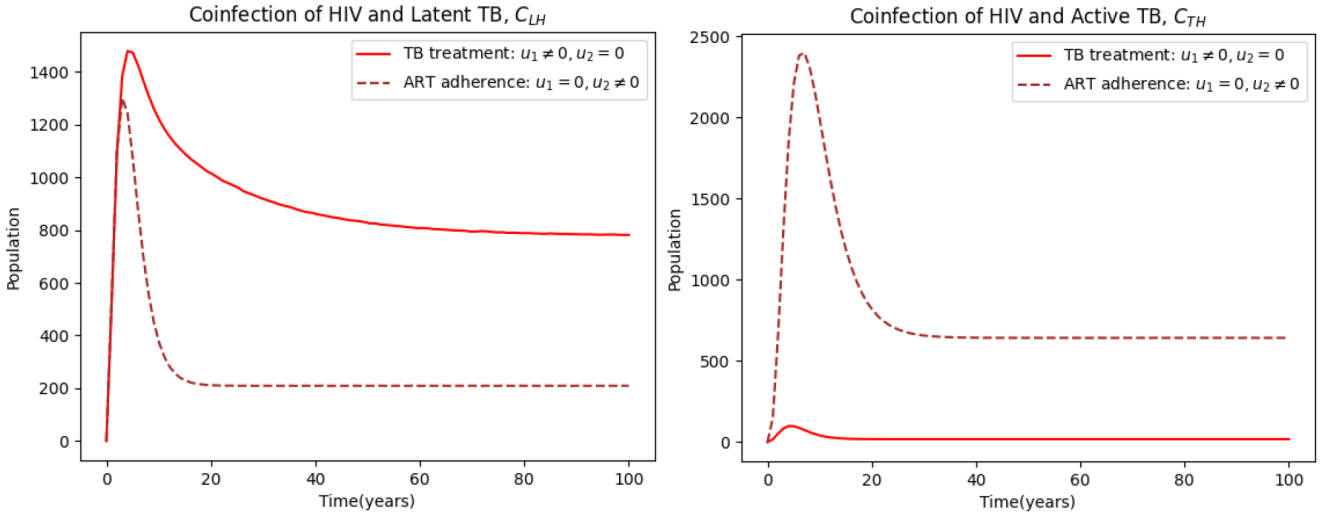

Figure 9. *Comparison between TB treatment only and ART adherence only strategies for the co-infection populations.*

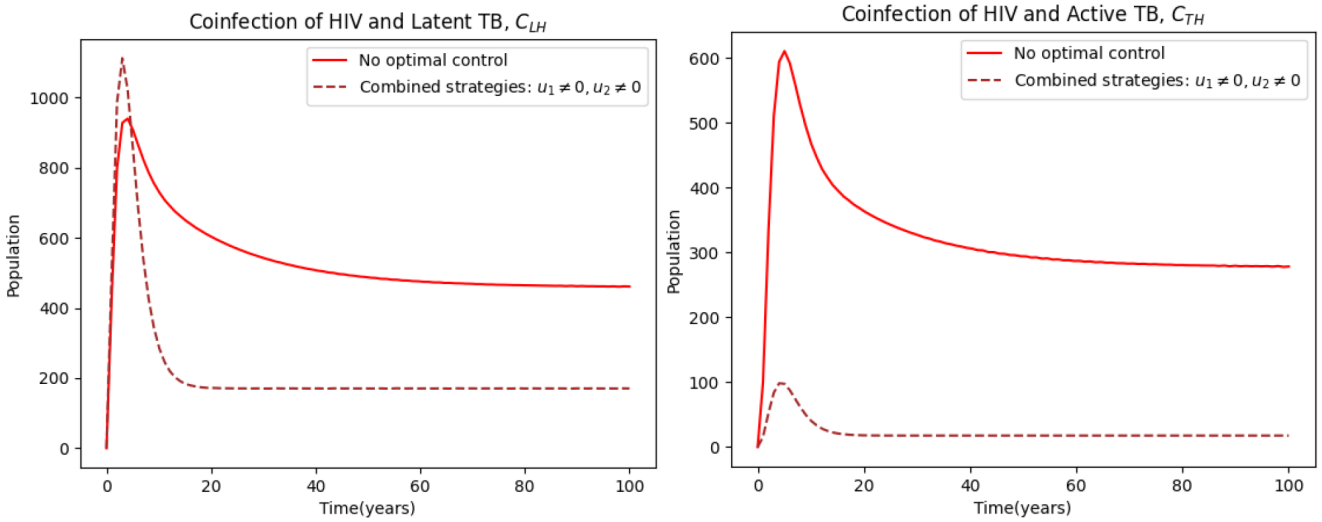

Figure 10. *Comparison between scenario when there is no optimal control and when there is optimal control: combined TB treatment and ART adherence strategies for the co-infection populations. of children.*

The controls also have great longterm significance in reducing, $C_{TH(i)}$ population size as displayed on the graph of 10-right.

3.7. Graphs for Adults, 15 Years & Above

In order to illustrate the feasibility of the theoretical results and the control strategies, graphs emanating from the numerical simulations are given. The python library, Matplotlib, is used to make the plots showing adults ($>$ 15 & above) population dynamics over time.

In figure 11, the HIV and TB submodel dynamics for adults are presented. It can be seen that in figure 11a that the susceptible population decreases drastically due to $R_0 = 2.238 > 1$. HIV undiagnosed, diagnosed and ART populations increase drastically in the initial 15 years. It can be noted that the population for the undiagnosed is lower compared to $D_i \& A_i$ populations due to the high rate of testing. All populations stabilize past 40 years.

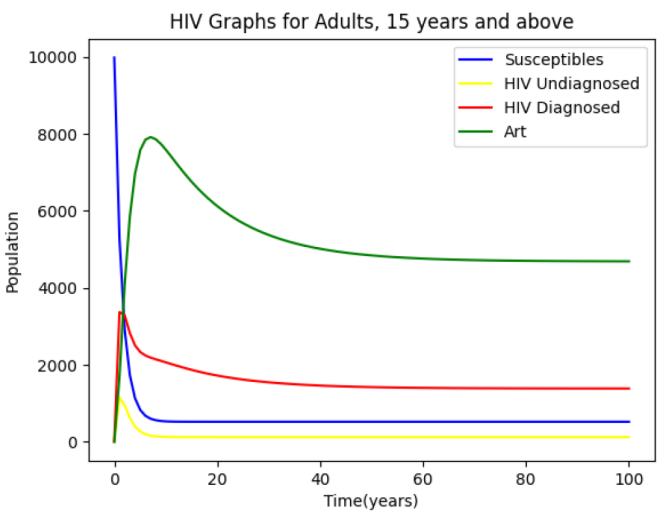

(a) HIV sub-model graphs for adults, 15 years & above.

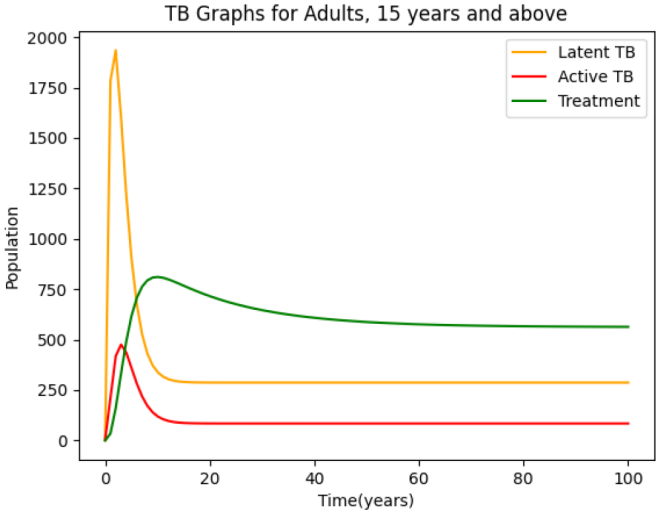

(b) TB sub-model graphs for adults, 15 years & above.

Figure 11. *Adults dynamics for sub-models.*

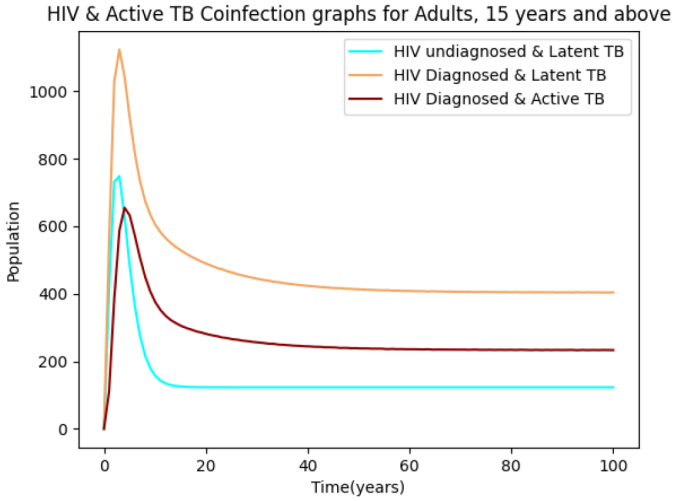

Figure 12. *Co-infection graphs for adults, 15 years & above.*

Figure 11b presents the dynamics for TB among adults. Latent and Active TB populations increases fast in the first 4 years but later it goes down to stabilize at about 10 years. TB treatment population increases over the first 10 years then it goes down slowly since the Active TB class has stabilized. There is minimum population change beyond 40 years.

The co-infection graphs for adults are presented by the figure 12. All thee three graphs increase to reach their maxima during the beginning 8 years then the populations decrease slowly to later stabilize past 40 years. Notably, the populations for co-infection of latent TB with undiagnosed HIV attains a higher maxima compared to the co-infection of latent TB and diagnosed HIV due to initializing the combined treatment at the rate, $\tau_{C(i)} = 0.65$.

On figure 13, an intervention comparison between viral load suppression and TB prevention are presented. While the graphs show explicitly that both the interventions reduce the co-infection adults population (Active TB and HIV), the simulations show that TB prevention is more effective for adults. Tuberculosis preventive therapy (TPT) significantly reduces the risk of TB and mortality. Since 2011, the World Health Organization recommends 3HP for PLHIV as part of routine HIV care [2]. 3HP is a TPT regimen which is endorsed by the WHO that combines high dose Isoniazid (H) and high dose rifapentine (P) once weekly for three months.

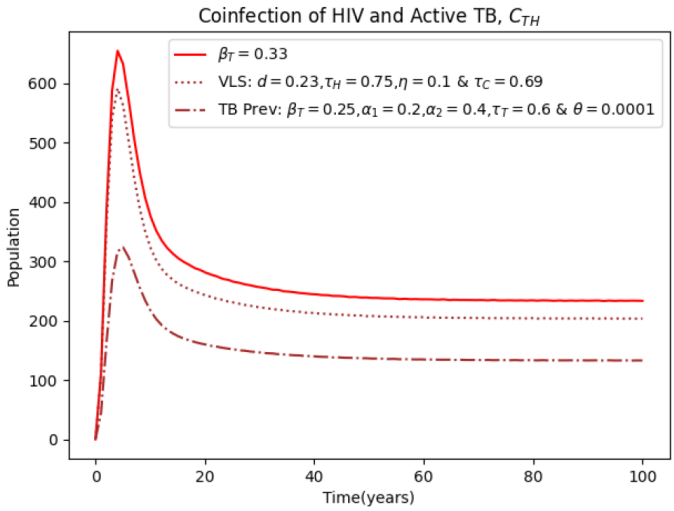

Figure 13. *Interventions comparison between viral load suppression and TB prevention on adults population.*

Figure 14 presents the coinfection population dynamics for adults considering the TB treatment and HIV adherence control interventions. The coinfections population sizes remain small due to intervention with controls. However, without controls, more people severely attacked with HIV & TB hence they progress to advanced stages so that the sizes of the coinfection populations population increases over time.

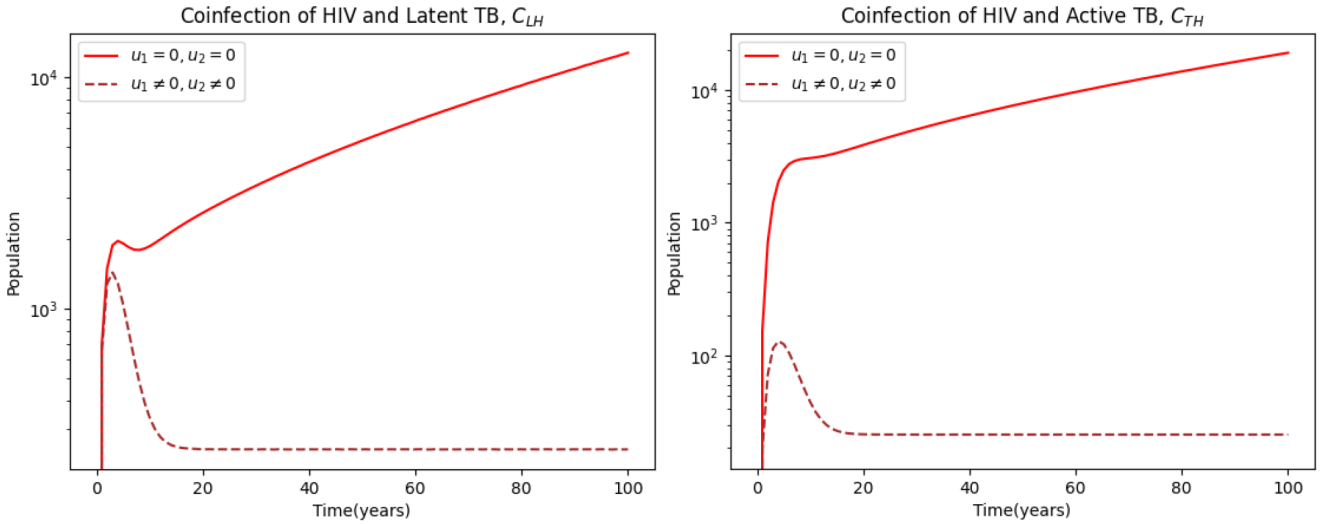

Figure 14. *Comparison of co-infection populations without and with control for adults (log-scale y-axis).*

Figure 15 compares the effect of the two control strategies in the coinfected populations. The graph on left shows that ART adherence is the most effective intervention for children infected with latent TB and HIV. TB treatment is the most effective intervention for children infected with active TB and HIV as shown in the graph or the right.

Figure 16 displays the comparison of the original coinfection dynamics presented at 12 with the dynamics with optimal control. The optimal controls do not have instant significance for coinfection of HIV and latent TB, $C_{LH(i)}$ population but have great longterm significance in reducing $C_{LH(i)}$ population size as displayed on the graph of 16-left. The optimal controls have instant and significance reduction for coinfection of HIV and active TB, $C_{TH(i)}$ population size.

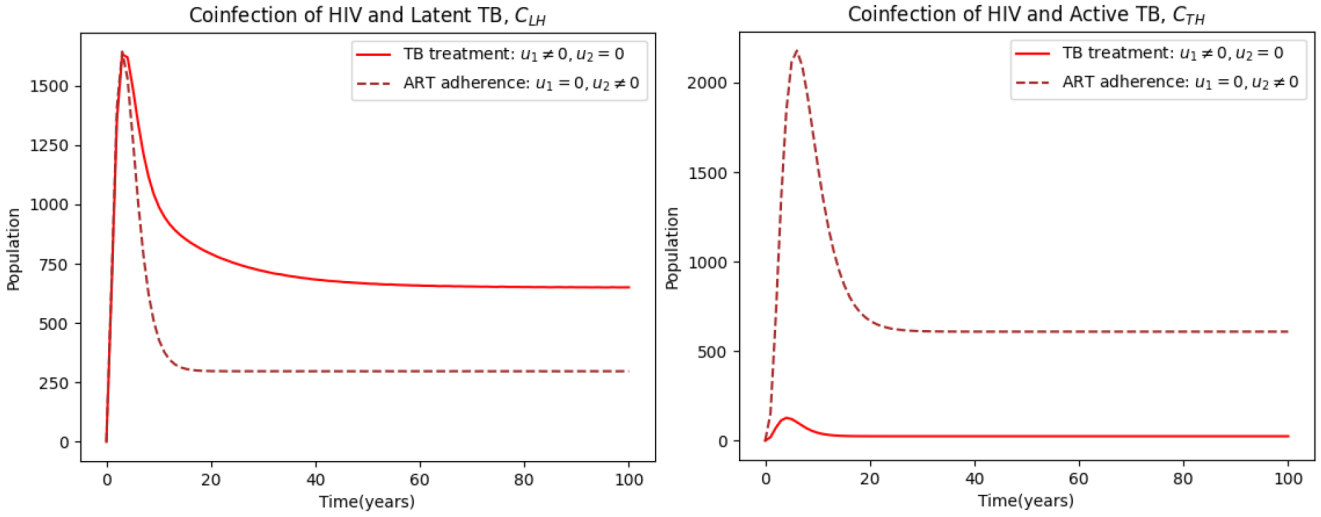

Figure 15. *Comparison between TB treatment only and ART adherence only strategies for the co-infection populations in adults population.*

The controls also have great longterm significance in reducing, $C_{TH(i)}$ population size as displayed on the graph of 16-right.

Throughout the simulations, it is also noted that HIV is more detrimental in adults than on children. This is the same with TB. However, figure 8 shows that if no control is done, children will be affected adversely by the coinfection compared to the adults as shown on the figure 14.

Numerical simulations results on the different interventions showed that ART treatment adherence lowers significantly the co-infection population in its earlier stages (HIV and latent TB). HIV treatment adherence prevents the progression of latent TB infection into active TB since HIV infection compromises the state of the person's immune system [29]. Thus, it is of paramount importance for latent TB coinfectives to be adhering to HIV treatment to prevent it from becoming active and consequently increasing the mortality rate of HIV patients.

It is also noted TB treatment reduces greatily the population of those affected with the coinfection on the later stage; both HIV and active TB coinfection.

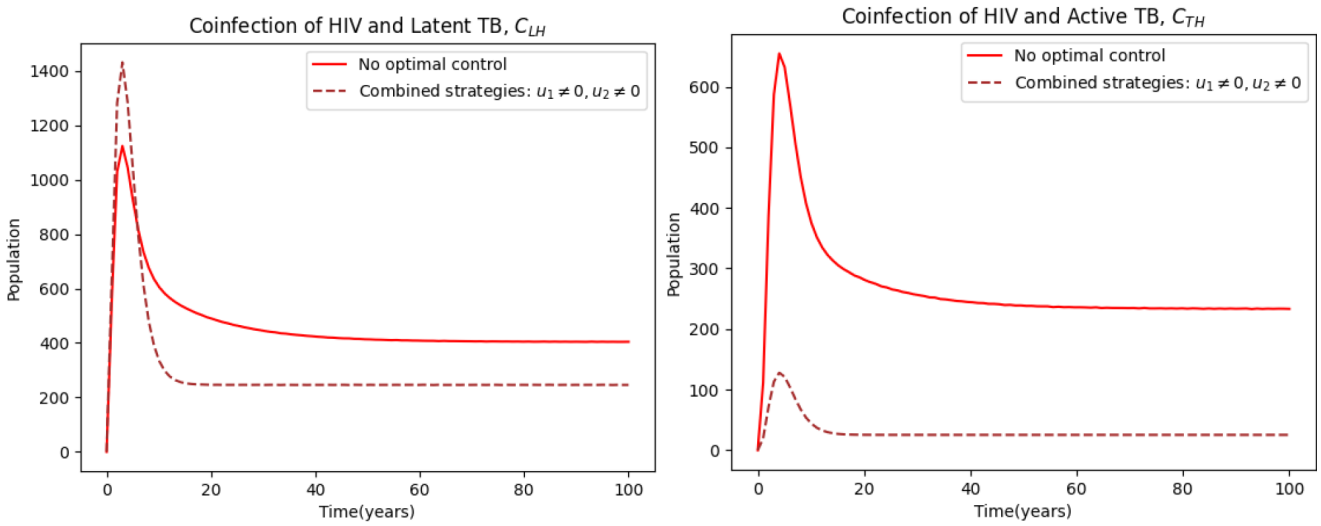

Figure 16. *Comparison between scenario when there is no optimal control and when there is optimal control: combined TB treatment and ART adherence strategies for the co-infection populations of children.*

TB treatment is important for people with HIV/TB coinfection because it can significantly improve their prognosis and reduce the risk of death [34]. TB can also worsen HIV progression by causing a rapid increase in HIV replication [35].

4. Conclusions

In this research, an age-stratified mathematical model for HIV and TB is developed and analyzed. Unlike the model in [24], this study considered two age groups; children (0-14 years) and adults ($>$ 15 years). HIV undiagnosed stage was also incorporated for the model.

This study proved that the formulated model is biologically and mathematically well posed on an invariant region Ω. HIV-free equilibrium and TB-free equilibrium is shown to be locally asymptotically stable by use of Ruorth-Hurtwiz criterion. The global stability of the HIV-free equilibrium and TB-free equilibrium is only guaranteed if the threshold quantity R_0^H and R_0^T is less than unity.

Viral load suppression is a more effective intervention for children compared to TB prevention. ART uptake should therefore be monitored for children to ensure achieving the necessary viral suppression level for children. On the other hand, TB prevention is a more effective intervention for adults compared to viral load suppression. TB preventative measures e.g. TPT, should therefore be emphasized in order to reduce HIV and active TB menace.

ART treatment adherence has proven to be the best intervention to control the co-infection in its earlier stages (HIV and latent TB). For ART to suppress HIV virus replication and remain effective over time, high levels of patient adherence are needed. The ministry should therefore invest in making ART treatment available for latent Tb coinfectives as well as enforcing combined treatment to the same. It is also noted TB treatment is the best intervention for those affected with the co-infection on the later stage; both HIV and active TB coinfection. It implies, adherence to HIV treatment alone, is not effective to control the coinfection.

HIV is more detrimental in adults than on children. This is the same with TB. However, if no control is done, children will be affected adversely by the coinfection compared to the adults. The health policy makers should therefore prioritize on elimination of mother to child transmission (eMTCT) of HIV.

One of the limitations of the study was inconsistency and non-linearity of the data used for data fitting. This study recommends assessing polynomial fitting, spline fitting, or other nonlinear models. The outliers data points should be determined if they are measurement errors or genuinely part of the data. Also, robust fitting techniques are recommended, like least absolute deviation or weighted least squares. This study recommends that more research should be done to ensure minimization of health risks of combining both treatments while eliminating the co-infection menace. Combining more than one intervention at a go is also recommended. More research could be done to consider the drug resistant TB. Finally, researchers could investigate on the cost effectiveness of different and/or combined interventions.

Symbols

S	Susceptible population
U	HIV undiagnosed population
D	HIV diagnosed population
A	Population on ART
E	Latent TB population
I	Active TB population
R	TB recovered population

C_{LU}	Latent TB and undiagnosed HIV co-infected population
C_{LH}	Latent TB and diagnosed HIV co-infected population
C_{TH}	Active TB and diagnosed HIV co-infected population
MOH	Ministry of Health
CDC	Centers for Disease Control
Par	Parameter
Desc	Description

Abbreviations

HIV	Human Immunodeficiency Virus
TB	Tuberculosis
VLS	Viral Load Suppression
ART	Antiretroviral Therapy
TPT	Tuberculosis Preventive Therapy
PLHIV	People Living with HIV
CLHIV	Children Living with HIV
DFE	Disease-Free Equilibrium
KENPHIA	Kenya Population-based HIV Impact Assessment
UNAIDS	United Nations Programme on HIV/AIDS

ORCID

0009-0007-0655-3393 (Robert Mureithi Maina)
0000-0002-9703-6514 (Samuel Musili Mwalili)
0000-0002-4447-2734 (Duncan Gathungu Kioi)

Author Contributions

Robert Mureithi Maina: Data curation, Project administration, Resources, Supervision

Mathew Ngugi Kinyanjui: Conceptualization, Data curation, Formal Analysis, Funding acquisition, Investigation, Methodology, Project administration, Resources, Software, Validation, Visualization, Writing - original draft, Writing - review & editing

Samuel Musili Mwalili: Conceptualization, Data curation, Formal Analysis, Funding acquisition, Investigation, Methodology, Project administration, Resources, Software, Validation, Visualization, Writing - original draft, Writing - review & editing

Duncan Gathungu Kioi: Conceptualization, Data curation, Formal Analysis, Funding acquisition, Investigation, Methodology, Project administration, Resources, Software, Validation, Visualization, Writing - original draft, Writing - review & editing

Conflicts of Interest

We declare we have no conflicts of interest.

References

[1] G. M. Shaw and E. Hunter, "Hiv transmission," Cold Spring Harbor perspectives in medicine, vol. 2, no. 11, p. a006965, 2012.

[2] WHO, Global health sector strategies on, respectively, HIV, viral hepatitis and sexually transmitted infections for the period 2022-2030. World Health Organization, 2022.

[3] CDC, Tuberculosis, TB. No. 33, Department of Health, Education, and Welfare, Public Health Service, Centerâ, 1977.

[4] NIH et al., "Hiv and opportunistic infections, coinfections, and conditions," 2022.

[5] WHO et al., "Who global lists of high burden countries for tuberculosis (tb), tb/hiv and multidrug/rifampicinresistant tb (mdr/rr-tb), 2021-2025: background document," Cold Spring Harbor perspectives in medicine, 2021.

[6] M. Amuyunzu-Nyamongo, "Hiv/aids in kenya: Moving beyond policy and rhetoric," African Sociological Review/Revue Africaine de Sociologie, vol. 5, no. 2, pp. 86-101, 2001.

[7] B. Tchakounte Youngui, B. K. Tchounga, S. M. Graham, and M. Bonnet, "Tuberculosis infection in children and adolescents," Pathogens, vol. 11, no. 12, p. 1512, 2022.

[8] G. G. Katana, M. Ngari, T. Maina, D. Sanga, and O. A. Abdullahi, "Tuberculosis poor treatment outcomes and its determinants in kilifi county, kenya: a retrospective cohort study from 2012 to 2019," Archives of Public Health, vol. 80, no. 1, pp. 1-13, 2022.

[9] S. Ali, A. A. Raina, J. Iqbal, and R. Mathur, "Mathematical modeling and stability analysis of hiv/aids-tb co-infection.," Palestine Journal of Mathematics, vol. 8, no. 2, 2019.

[10] T. Getaneh, A. Negesse, G. Dessie, and M. Desta, "The impact of tuberculosis co-infection on virological failure among adults living with hiv in ethiopia: A systematic review and meta-analysis," Journal of Clinical Tuberculosis and Other Mycobacterial Diseases, vol. 27, p. 100310, 2022.

[11] K. KENPHIA, "Kenya population-based hiv impact assessment," Kenya Population-based HIV Impact Assessment. Accessed August 2022, vol. 14, 2022.

[12] S. Klemm and L. Ravera, "On sir-type epidemiological models and population heterogeneity effects," Physica A: Statistical Mechanics and its Applications, vol. 624, p. 128928, 2023.

[13] C. Ozcaglar, A. Shabbeer, S. L. Vandenberg, B. Yener, and K. P. Bennett, "Epidemiological models of mycobacterium tuberculosis complex infections," Mathematical biosciences, vol. 236, no. 2, pp. 77-96, 2012.

[14] C. Walker, "Well-posedness and stability analysis of an epidemic model with infection age and spatial diffusion," Journal of Mathematical Biology, vol. 87, no. 3, p. 52, 2023.

[15] P. Van den Driessche and J. Watmough, "Reproduction numbers and sub-threshold endemic equilibria for compartmental models of disease transmission," Mathematical biosciences, vol. 180, no. 1-2, pp. 29-48, 2002.

[16] R. Devaney, An introduction to chaotic dynamical systems. CRC press, 2018.

[17] E. X. DeJesus and C. Kaufman, "Routh-hurwitz criterion in the examination of eigenvalues of a system of nonlinear ordinary differential equations," Physical Review A, vol. 35, no. 12, p. 5288, 1987.

[18] T. O. Orwa, R. W. Mbogo, and L. S. Luboobi, "Mathematical model for hepatocytic-erythrocytic dynamics of malaria," International Journal of Mathematics and Mathematical Sciences, vol. 2018, no. 1, p. 7019868, 2018.

[19] T. O. Orwa, R. W. Mbogo, and L. S. Luboobi, "Multiplestrain malaria infection and its impacts on plasmodium falciparum resistance to antimalarial therapy: A mathematical modelling perspective," Computational and Mathematical Methods in Medicine, vol. 2019, no. 1, p. 9783986, 2019.

[20] P. Van den Driessche and J. Watmough, "Further notes on the basic reproduction number," Mathematical epidemiology, pp. 159-178, 2008.

[21] M. Zamir, G. Zaman, and A. S. Alshomrani, "Sensitivity analysis and optimal control of anthroponotic cutaneous leishmania," PloS one, vol. 11, no. 8, p. e0160513, 2016.

[22] M. Das, G. Samanta, and M. De la Sen, "A fractional ordered covid-19 model incorporating comorbidity and vaccination," Mathematics, vol. 9, no. 21, p. 2806, 2021.

[23] N. Chitnis, J. M. Hyman, and J. M. Cushing, "Determining important parameters in the spread of malaria through the sensitivity analysis of a mathematical model," Bulletin of mathematical biology, vol. 70, pp. 1272-1296, 2008.

[24] R. Aggarwal and Y. A. Raj, "A fractional order hivtb co-infection model in the presence of exogenous reinfection and recurrent tb," Nonlinear Dynamics, vol. 104, pp. 4701-4725, 2021.

[25] "World Bank Open Data," 2022. [Accessed 29-11-2024].

[26] E. Omondi, R. Mbogo, and L. Luboobi, "Mathematical modelling of the impact of testing, treatment and control of hiv transmission in kenya," Cogent Mathematics & Statistics, vol. 5, no. 1, p. 1475590, 2018.

[27] O. B. VINCENT, "A mathematical model of hiv and tb co-infection with interventions, a case of siaya county in kenya," 2022.

[28] A. S. Ajiboye, "Tuberculosis preventive treatment updateâus presidentâs emergency plan for aids relief, 36 countries, 2016-2023," MMWR. Morbidity and Mortality Weekly Report, vol. 73, 2024.

[29] L. B. Whiteley, E. M. Olsen, K. K. Haubrick, E. Odoom, N. Tarantino, and L. K. Brown, "A review of interventions to enhance hiv medication adherence," Current Hiv/Aids Reports, vol. 18, no. 5, pp. 443-457, 2021.

[30] T. K. Ayele, E. F. D. Goufo, and S. Mugisha, "Mathematical modeling of hiv/aids with optimal control: a case study in ethiopia," Results in Physics, vol. 26, p. 104263, 2021.

[31] K. R. Cheneke, "Optimal control and bifurcation analysis of hiv model," Computational and Mathematical Methods in Medicine, vol. 2023, no. 1, p. 4754426, 2023.

[32] L. Pontryagin et al., "The mathematical theory of optimal processes,(1962), chap. 2," VI, JohnWilely & Sons, 1962.

[33] R. C. Patel, P. Oyaro, B. Odeny, I. Mukui, K. K. Thomas, M. Sharma, J. Wagude, E. Kinywa, F. Oluoch, F. Odhiambo, et al., "Optimizing viral load suppression in kenyan children on antiretroviral therapy (opt4kids)," Contemporary Clinical Trials Communications, vol. 20, p. 100673, 2020.

[34] I. Navasardyan, R. Miwalian, A. Petrosyan, S. Yeganyan, and V. Venketaraman, "Hiv-tb coinfection: Current therapeutic approaches and drug interactions," Viruses, vol. 16, no. 3, p. 321, 2024.

[35] A. Bhatt, Z. Q. Syed, and H. Singh, "Converging epidemics: A narrative review of tuberculosis (tb) and human immunodeficiency virus (hiv) coinfection," Cureus, vol. 15, no. 10, 2023.